Effects of KNO_3 and NaH_2PO_4 on Lipid Synthesis and $CaCO_3$ Accumulation in *Pleurochrysis carterae* and Newly Identified Algal Shell Coccolith Structure

A thesis presented to

The Faculty of Graduate Studies

Lakehead University

Submitted by

XUANTONG CHEN

In partial fulfillment of requirements for the degree of

[Master of Science in Forestry]

Thunder Bay, Ontario, Canada, 2019

ABSTRACT

Due to the limited energy reserves and the increasing demand for energy, a large number of greenhouse gases such as CO_2 have been released to the air. Therefore, there is an urgent need to find new sources of energy and ways which can effectively fix carbon dioxide. *Pleurochrysis carterae*, a marine microalga is considered a potential biodiesel producer and an effective carbon dioxide fixer, due to its high lipid content (33% of dry weight) and a unique calcification process. However, the current research on *P. carterae* is very limited. In my research, the effects of NaH_2PO_4 and KON_3 on *P. carterae* were studied; furthermore, the novel coccolith structure was also discovered. From the results of the effect of NaH_2PO_4 on *P. carterae*, *P. carterae* reached the maximum cell number ($32.67\times10^5\cdot mL^{-1}$) on day 22 under 1.5 mM of NaH_2PO_4. Furthermore, when the concentration of NaH_2PO_4 in the medium is higher than control, it could induce *P. carterae* to secrete acidic substances to lower the pH in the medium. The highest calcium content of *P. carterae* is 7.26% with 0.5 mM of NaH_2PO_4 in the medium on day 10. Furthermore, the higher concentration of NaH_2PO_4 could inhibit the calcification. The lipid accumulation is negatively correlated with NaH_2PO_4 concentration. The highest chlorophyll α content is 6.37 $mg\cdot L^{-1}$ on day 26 with 2mM of NaH_2PO_4. Examining the effect of KNO_3 on *P. carterae*, we found that under 0.75 $mmol\cdot L^{-1}$ of KNO_3, *P. carterae* has the highest calcium carbonate content (10.01%) and the largest cell size. The highest lipid content (33.61% of dry weight) was shown in the control group (0 $mmol\cdot L^{-1}$). Furthermore, the lipid and carbohydrate content is negatively correlated to the concentration of KNO_3. *P. carterae* has the highest protein content of 32.87% with 1 $mmol\cdot L^{-1}$ of KNO_3 on day 10. The FTIR results are consistent with the increase of protein

and decrease of lipids and carbohydrate. In this research, the novel coccolith structures of *P. carterae* were also discovered. We observed a new structure in the inner tube of the R unit and named as “doornail structure”, which is also parallel with the outer tube of the V unit. The “doornail structure” makes the coccolith more stable and not easily broken. Moreover, we first observed a complete coccoliths shell structure. From SEM result, the double-disc of adjacent coccoliths cross each other, and such a cross-structure ensures that each coccolith cannot move freely in a horizontal direction. Therefore, each coccolith is fixed to form a support structure. Furthermore, this cross-structure can be stretched and not damaged by the expansion of the protoplasts during the division of the cell. This is the first research that revealing how coccolith protects and supports the *P. carterae* cells.

Keywords: *Pleurochrysis carterae*, Coccolith, Lipid, Chlorophyll, Protein, Carbohydrate, Doornail structure, Cross structure

ACKNOWLEDGEMENTS

I would like to express my sincere gratitude to honorable supervisor Dr. Wensheng Qin for his generosity, encouragement and patient guidance during my MSc study and other related research projects. I am very grateful to him for giving me this opportunity to study at Lakehead University, which really changed my whole life.

I would also like to thank my supervisory committee members: Dr. Brian Ross, Dr. Robert Mackereth and external examiner Dr. Baoqiang Liao, for their insightful comments in wider perspectives of research which provide me encouragement for future research endeavor. I also would like to thank the program coordinator Dr. Brian McLaren for his help during my whole Master's studies. I thank Dr. Guosheng Wu for his helping me in SEM examination and imaging; I also thank other professors and graduate students at Lakehead University for their valuable suggestions and comments during my studies, especially Dr. Susanne Wolford, Michael Moore and Michael Sorokopud.

I am thankful to all my lab members for their help and suggestions on my research. And finally I would like to thank my parents for supporting my study aboard, and sincerely extend my appreciation to my wife and my other family members for their great motivation and understanding.

TABLE OF CONTENTS

LIST OF TABLES

CHAPTER III

CHAPTER V

LIST OF FIGURES

CHAPTER I

CHAPTER II

CHAPTER III

CHAPTER IV

CHAPTER V

CHAPTER I

An Overview of Marine Microalgae *Pleurochrysis carterae*

Abstract

As the global industrialization accelerates process, the demand for fuel and greenhouse gas emissions are increasing dramatically, especially the amount of carbon dioxide. To solve this series of problems, humans began to look for new, alternative energy sources, such as bioethanol, biodiesel. To reduce carbon dioxide in the environment, chemical immobilization, physical fixation, or biofixation are used. Among them, microalga is generally considered to be most effective because of its faster growth rate, wider distribution range, and lower cost. *Pleurochrysis carterae* is a marine microalga that not only absorbs carbon dioxide by photosynthesis but also absorbs HCO_3^- in the ocean and air to synthesize $CaCO_3$ through its unique calcification. Moreover, *Pleurochrysis carterae* has a lipid content as high as to 33 %, which also contains docosahexaenoic acid (DHA) with high nutritional value. In other words, *Pleurochrysis carterae* not only has a high potential value in fixing carbon dioxide but also has great potential in the production of biodiesel and biomedicine.

Key words： *Pleurochrysis carterae*, Calcium, Lipid

1. Introduction

With the acceleration of global industrialization, humans are increasing the demand for energy. Before the industrial revolution, the concentration of carbon dioxide in the atmosphere was maintained at 280 ppm. However, by the end of the twentieth century, the concentration of carbon dioxide in the atmosphere had increased to 367 ppm and showed a continuous and rapid increasing (Geider et al. 2001; Le Quéré et al. 2012). The global warming effect has already begun to appear due to the increase in greenhouse gas content such as CO_2 (Cox et al. 2000). Among all potential greenhouse gases, carbon dioxide is considered to be one of the major reasons for global warming. To reduce the content of carbon dioxide in the atmosphere, there are three main ways: 1. Improve energy efficiency and reduce energy use to achieve emission reduction. 2. Develop new energy sources such as nuclear energy, wind energy, and solar energy. 3. Fix carbon dioxide or convert it to other collectible chemicals.

Compare to improve energy efficiency and develop new energy sources，to fix or convert carbon dioxide is more environment-friendly and cheaper. There are currently three main technical means for fixing and converting methods：(1) Chemical fixation: using an absorbent such as sodium carbonate, potassium carbonate solution (Meisen and Shuai 1997); or using CO_2 with hydrogen, methane and water to synthesize methanol and other chemicals (Jia et al. 2004). However, the problem is that the use of chemical methods to fix carbon dioxide requires a higher purity of carbon dioxide, which increases the cost and is not suitable for promotion. (2) Physical fixation: Using certain solid materials to adsorb carbon dioxide (Meisen and Shuai 1997) or by liquefying carbon dioxide, it can be

buried underground (Ohsumi 2004). The disadvantage of these methods is also that it is difficult to promote due to the high cost. (3) Biofixation: Using photosynthesis and calcification of an organism to absorb and fix the carbon dioxide (Benemann 1997; Hase et al. 2000). Biofixation is widely available on the planet and is the safest, most efficient and cost-effective method of carbon sequestration.

The organisms capable of carbon dioxide fixation mainly include plants, bacteria, and algae. Compared with other carbon-fixing organisms, algae have a higher growth rate, photosynthesis efficiency, and CO_2 fixation rate, so it is regarded as a potential carbon-fixing organism (Benemann 1997; Packer 2009). As a single-cell marine microalga, *Pleurochrysis carterae* can absorb carbon dioxide from the surrounding environment for photosynthesis and produce organic substances such as proteins and lipids; it can also convert carbon dioxide into the outer shell of calcium carbonate by calcification. Therefore, *P. carterae* has a broad application prospect in fixing carbon dioxide.

2. *Pleurochrysis carterae*

Pleurochrysis carterae, also known as coccolithophorid, belongs to Haptophyta and is important to marine phytoplankton (Paasche 1968). *P. carterae* are light-energy autotrophic unicellular algae. The cells are mostly round or elliptical and contain two chloroplasts (Daugbjerg and Andersen 1997). The cell surface is covered with a shell composed of calcium carbonate (Marsh 2003). Like most photoautotrophs, *P. carterae* can synthesize organic matter through photosynthesis, providing substances and energy for growth and reproduction. *P. carterae* also has a special biological calcification process.

P. carterae forms a $CaCO_3$ scaly structure called coccolith on the surface of its cells by calcification (Marsh 2003). Because of its unique calcification process, *P. carterae* together with foraminifera, coral reefs, etc. constitute the main biological part source of the marine inorganic carbon cycle (Brownlee and Taylor 2004).

2.1 Growth and life-cycle of *Pleurochrysis carterae*

P. carterae cells are vegetatively propagated using binary fission. After the cell division is completed, the daughter cells synthesize a coccolith on the cell surface through calcification. *P. carterae* has two cell states, swimming and non-swimming. Previous research found that cells in both states can vegetatively propagate (Leadbeater and Green 1994). Current research on the life cycle of coccolithophorid focuses on *Emiliania huxleyi.* There are mainly three types of cell morphology during the growth process of *E. huxleyi*: C type, N-type and S type (Klaveness and Paasche 1971). Type C has coccolith but no flagella, therefore it cannot swim; Type N has no coccolith and no flagella; Type S has coccolith and flagella (Paasche 1967). These three types of cells all reproduce in the form of binary fission (Paasche 2001).

The surface of calcified coccolithophore cells is often coated with a single layer (e.g., *Pleurochrysis carterae*) or multiple layers (e.g., *E. huxleyi*) of coccolith. The coccolith is mostly elliptical, 1 to 20 μm, composed of calcite and a small amount of organic matter (Paasche 1968). At present, there is no unified opinion on why the coccolith exists on the surface of coccolithophore cells. There are many hypotheses (Brand 2006; Sikes et al. 1980): (1) Reduces the inhibition of cells due to the strong light when the cell is illuminated; (2) In low light conditions, light is focused on the chloroplast by refraction to

ensure the need for photosynthesis; (3) Increase cell volume; (4) Cell self-protection; (5) Increase cell sedimentation rate.

2.2 Coccolithophore and ecology

Coccolithophore is widely distributed in tropical and temperate oceans, and even in some areas, it is the major components of plankton (Jeffrey and Allen 1964). Some studies have suggested that coccolithophore can occupy an important position in the marine ecosystem, which is related to the ability of the algae to secrete certain toxins (Houdan et al. 2004). *P. carterae* can produce dimethylsulfoniopropionate (DMSP), and the DMSP has been shown to inhibit bacteria, algae, protozoans and fungi (Malin and Erst 1997; Sieburth 1960; Sverdrup et al. 2001; Van Alstyne and Houser 2003).

In Arctic waters, the biodiversity of coccolithophore is much lower than in subtropical waters (Hulburt 1963; McIntyre 1967). In inland freshwaters, coccolithophore is also rare; *hymenomona roseola* is one of the few known freshwater algae species (Johansen et al. 1988). Like most plankton, coccolithophore generally lives in areas with a strong light to use sunlight for photosynthesis. Coccolithophore could easily form water blooms in a suitable environment (Blackburn and Cresswell 1993; Zhou et al. 2008a).

Because of the unique physiological and biochemical properties of coccolithophore, it has an important impact on global climate and marine ecosystems. The coccolith on the surface of coccolithophore has certain optical properties; it can enhance ocean reflectivity, reduces radiation intensity, and thus affects the change of earth surface temperature (Tyrrell et al. 1999). Also, coccolithophore has a higher yield of dimethyl sulfide (DMS), and dimethyl sulfide is the main source of cloud condensation nuclei, a large number of

DMS could change the reflectivity of the cloud, affecting global temperatures (Keller 1989). In the coccolithophore cells, there are two processes in which photosynthesis converts CO_2 into organic carbon (Formula 1) and calcification converts HCO_3^- into CO_2 (Formula 2) and these two opposite processes have an important impact on the changes in CO_2 in the ocean surface and profoundly affect the deposition of marine carbonates (Rost and Riebesell 2004).

$$CO_2 + H_2O = CH_2O + O_2\uparrow \qquad \text{Formula 1}$$

$$Ca^{2+} + 2HCO_3^- = CaCO_3\downarrow + H_2O + CO_2\uparrow \qquad \text{Formula 2}$$

At the same time, coccolithophore is the highest marine primary producer and plays an important role in the composition of the marine food chain.

2.3 Photosynthesis and calcification of coccolithophore

Biocalcification is a very common phenomenon, and many kinds of organisms can be calcified, such as coccolithophore, foraminifera, polyps (Ehrlich 1998). Algae are capable of calcification include cyanobacteria, green and brown algae. Calcification is a chemical process which is affected by many factors such as calcium ion concentration, inorganic carbon concentration, pH value and nucleation sites (Gattuso and Buddemeier 2000).

2.3.1 Coccolith structure

The coccoliths of *Pleurochrysis carterae* are composed of a distal rim of interlocking $CaCO_3$ crystals with an oval organic base plate (Fig. 1) (Marsh 2003). The coccolith consists mainly of two parts, V unit and R unit (Young and Bown 1991); outer-tube and distant-shield elements form the V unit (Fig. 1) and the R unit is a combination of the inner tube and proximal-shield (Fig. 1). The closed double disc construction is formed by

alternating V unit and R unit combined on the organic base plate; moreover, the V unit and R unit are not inter-grown, just interlocking (Marsh 1994).

Regarding the structure of the V unit and the R unit, the angle between the outer unit of the V unit and the base plate is 60°; the distant-shield is almost parallel to the base plate. The proximal-shield of R unit is attached to the base plate and parallel to it; the inner-tube of R unit is inwardly angled to the base plate by approximately 50° (Marsh 1999a).

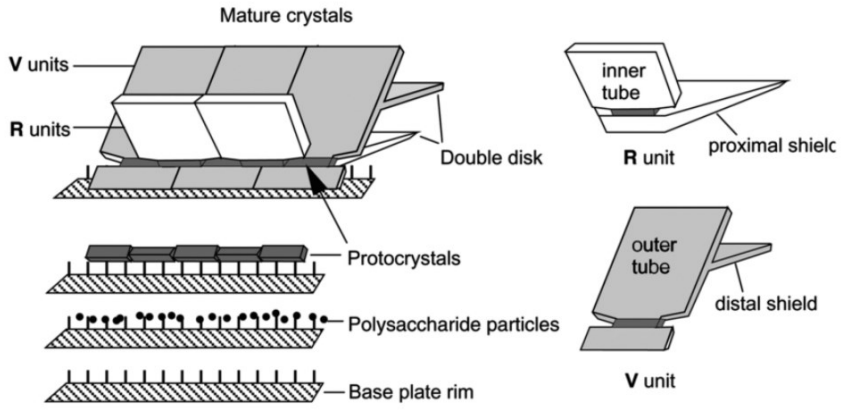

Fig. 1 Coccolith structure of *P. carterae* (Marsh 2003)

2.3.2 Coccolith formation process

In *P. carterae* the base plates and acidic polysaccharides of coccoliths are synthesized in Golgi cisternae then transfer to the mineralizing vesicle for calcite rims fabrication (Fig.2) (de Vrind-de Jong and de Vrind 1997; Marsh 2003). Before mineral deposition, 20 nm particles (formed by two acidic polysaccharides PS1 and PS2) with calcium ions are attached to the base plate rim (Marsh 1994; Outka and Williams 1971a; Van der Wal et al. 1983). PS2 is a high-capacity calcium binding acidic polysaccharide. The major function of PS2 is to buffer the calcium ion concentration in the mineralizing vesicle. However, the growth process of coccolith requires acidic polysaccharides PS3; it is located in the interface between the growing crystals. The major function of PS3 is that it is responsible

for the regulation of mineralization after the synthesis of *protococcolith* ring (Marsh 2003). After the action of PS1, PS2 and PS3, coccolith is released to the cell surface by Golgi vesicles.

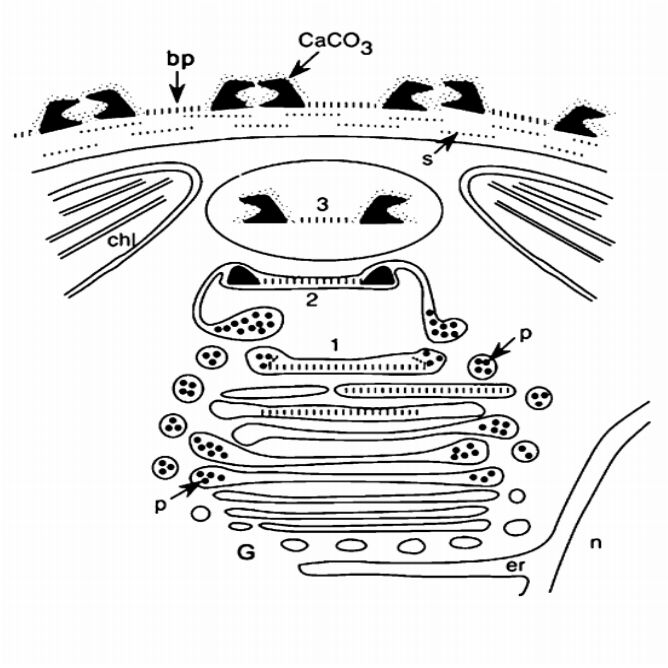

Fig. 2 Coccolith formation pathway in *Pleurochrysis carterae* (Marsh 1994). There are three successive stages in mineralizing vesicles are showed. **(1)** $CaCO_3$ deposition. **(2)** Crystal growth. **(3)** After cessation of crystal growth. **(p)** Acidic polysaccharides PS2-containing particles mediate mineralization. **(bp)** Base plates **(chl)** Chloroplasts **(G)** Golgi stacks **(er)** Endoplasmic reticulum **(n)** Nucleus **(s)** unmineralized scales

2.3.3 Photosynthesis - Calcification coupling model

Coccolithophore fixes inorganic carbon by cell photosynthesis and calcification. Previous studies have found that in many calcified algae, calcification and photosynthesis are coupled (Borowitzka and Larkum 1987). In general, the concentration of CO_2 in seawater is maintained at 5 ~ 25 μmol/L, which does not meet the demand for ribulose-1, 5-bisphosphate carboxylase oxygenase (Rubisco). Phytoplankton supplements

intracellular CO_2 concentration by calcification to meet the needs of photosynthesis. However, the CO_2 concentration mechanism of coccolithophore is relatively inefficient and often does not meet Rubisco's demand for CO_2. At this time, coccolithophore can supplement CO_2 of intracellular cells by calcification to ensure the normal operation of photosynthesis (Nimer and Merrett 1993; Sikes and Wilbur 1980). At present, the research on the relationship between photosynthesis and calcification is mainly concentrated in *E. huxleyi*, and several models are proposed to explain the correlation of photosynthesis-calcification in coccolithophore cells (Brownlee 1994; Paasche 1964, 2001; Shiraiwa 2003; Sikes and Wilbur 1980). Currently, the widely accepted photosynthesis-calcification coupling model was proposed by Borowitzka (Borowitzka 1989) and later modified by Raven (Raven 1997) (Fig.3).

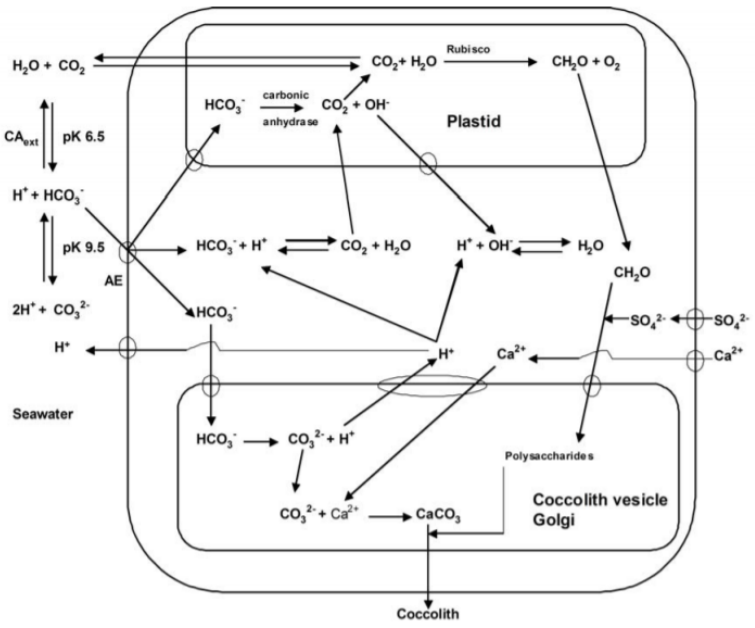

Fig. 3 The most accepted photosynthesis - calcification coupling model cited from (Moheimani 2005)

In this model, HCO_3^- acts as a carbon source for cell calcification and photosynthesis,

which forms OH^- through photosynthesis and produces H^+ through calcification. Neutralization of OH^- and H^+ maintains the pH inside the cytoplasm at around 7. Moreover, in this model, the CO_2 formed inside the cells can be transferred to the outside of the cells, which can also be a supplement for some of the inorganic carbon sources consumed in the culture solution due to cell photosynthesis and calcification.

2.4 Lipids in *Pleurochrysis carterae*

Cardiovascular disease (CVD) is the leading cause of death in the world (Surette et al. 2004). Consumption of fish oil which rich in ω-3 polyunsaturated fatty acids (PUFAs) such as eicosapentaenoic acid (EPA, 20:5 ω- 3) and docosahexaenoic acid (DHA, 22:6 ω-3) has been shown that it can reduce the extent of CVD (Simopoulos 2002). Moreover, when PUFAs combined with γ-linolenic acid (GLA, 18:3 ω-6), it has been shown to reduce the risk of chronic inflammatory disorders such as asthma and rheumatoid arthritis (RA). GLA plays a key role in the anti-inflammatory responses by inhibiting the generation of pro-inflammatory leukotriene B4 and its precursors (Chilton et al. 2008; Garcia de Acilu et al. 2015). However, fish oil contains very little GLA. GLA exists only in the seed oil of plants and some blue algae. The currently best-known routes for DHA biosynthesis are depicted in a simplified form as shown in Figure 4 (Meyer et al. 2004).

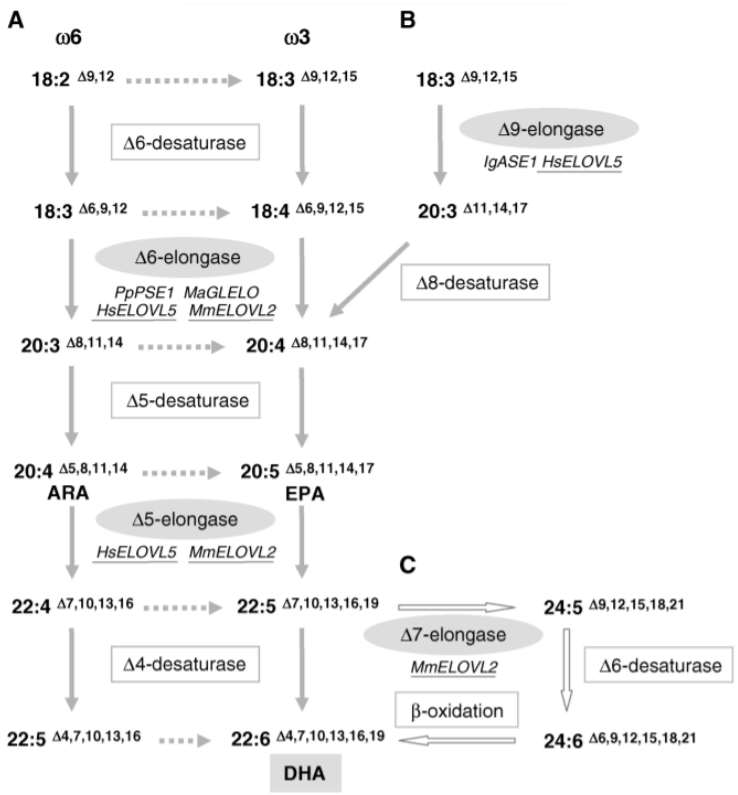

Fig. 4 The pathways of ω6 and ω3 for long-chain polyunsaturated fatty acids synthesis in eukaryotes (Meyer et al. 2004). The desaturases and elongases consecutive action can convert ω6-18:2 and ω3-18:3 to docosahexaenoic acid (DHA), can starting at Δ6 desaturation (**A**) orΔ9 elongation (**B**). The dash arrows (ω3-desaturases) link the ω6 and ω3 pathway in most of the eukaryotes, which are missing in mammals. The cloned elongases examples were involved in DHA synthesis was shown in the figure. Some single step has their specific elongases, such as the moss PpPSE1 and the fungal MaGLELO. Others are nonspecific, such as the human HsELOVL5 and the murine MmELOVL2; underlined.

Marine microalgae have been considered the most viable alternative to fish oil as a natural source of PUFAs (Rodolfi et al. 2009). *Nannochloropsis spp., Isochrysis galbana* and *phaedactylum tricornutum* have been demonstrated to produce EPA and DHA, but

the biomass production is very low (Wen and Chen 2003).

The *P. carterae* cells can also accumulate large amounts of oil reaching 33% of the dried cell weight (Moheimani and Borowitzka 2006). It has been described that *P.carterae* is an ideal candidate for simultaneous production of EPA, DHA and GLA as human food supplements. An added benefit of consuming *P.carterae* is the concomitant intake of $CaCO_3$ which can supplement calcium for anti-osteoporosis purposes because the role of calcium in preventing osteoporosis has been widely appreciated (Galli et al. 2014; Reginster 1995; Schröder et al. 2012; Wadolowska et al. 2013).

3. The application of microalgae

The history of human use of microalgae dates back to 2000 when edible blue-green algae such as *Nostoc, Arthrospira* and *Aphanizomenon* were used as food (Jensen 2001). The development of microalgae biotechnology began in the mid-20th century. At present, there are a large number of commercial applications of microalgae: (1) Because of the special components contained in algae cells; microalgae are often used as functional foods with high nutritional value; (2) For aquaculture, or as animal feed; (3) Application and cosmetics industry. Some algae cells are used in infant nutrition formula because they contain polyunsaturated fatty acids (PUFA). Microalgae pigments are also considered as high-value natural dyes (Spolaore et al. 2006). It is estimated that the current global demand amounts to 5,000 tons of dry algae powder per year, which is about $1.25 billion per year (Pulz and Gross 2004). Currently, the microalgae that have been used for large-scale commercial applications include *Arthrospirea, Chlorella, Dunaliella salina* and *Aphanizomenon flos-aquae*.

3.1 The application of *Pleurochrysis carterae*

P. carterae not only absorbs carbon dioxide for photosynthesis but also produces organic substances. Moreover, *P. carterae* can accumulate $CaCO_3$ on the cell surface to form the coccolith. Previous research found that the content of $CaCO_3$ on the surface of *P. carterae* cells can reach 10% of the dry algal weight, and the content of intracellular lipids can reach 33% of the dry algal weight (Moheimani and Borowitzka 2006). Moreover, *P. carterae*'s lipids are rich in long-chain unsaturated fatty acids DHA (22:6ω-3, docosahexaenoic acid), and its DHA accounts for 30% ~ 40% of total fatty acid content (Bell and Pond 1996). DHA has a wide range of uses in the prevention and treatment of cardiovascular diseases and infant foods, with global market demand of billions of dollars. Therefore, it is no doubt that *P. carterae* has broad commercial prospects.

3.1.1 CO_2 reduction

The inevitable result of the massive use of fossil fuels such as coal, crude oil and natural gas by humans is the release of carbon dioxide into the air, which is particularly significant in the chemical industry, coal power generation, transportation and residential life. The release of carbon dioxide and its large accumulation in the air have been identified as the main cause of global warming. At present, the annual global carbon dioxide emissions are about 30 billion tons and are increasing at a rate of 3% per year (Metz et al. 2005).

Microalgae have been widely recognized as the most effective natural system for capturing carbon dioxide because they have a more effective photosynthesis system than conventional crops. Microalgae can absorb more carbon dioxide and convert it into

organic matter such as sugar and starch and produce a large amount of oxygen. Some microalgae species can accumulate a large number of oils and fats in the cells while fixing the carbon dioxide. These lipids can be processed into various types of renewable biofuels, such as biodiesel, and aviation kerosene. (Gao and McKinley 1994; Hossain et al. 2008; Schenk et al. 2008).

Compared to other alga species, coccolithophore has shown greater efficiency in reducing carbon dioxide emissions. It not only converts carbon dioxide into organic matter through photosynthesis but also converts carbon dioxide into $CaCO_3$ through calcification. It is estimated that coccolithophore absorbs CO_2 7.33×10^{11} tons per year, fixes carbon 2.00×10^{11} tons, and produces $CaCO_3$ 1.28×10^{9} tons. Its $CaCO_3$ production accounts for about half of the world's total production in nature (Buitenhuis et al. 1999).

3.1.2 Biomedical materials

The coccolith formed on the coccolithophore cell surface by calcification, mainly composed of $CaCO_3$ and a small amount of organic matter, has good biocompatibility. Also, coccolith undergoes a complex folding process during its formation, which results in a higher surface area to volume ratio and is, therefore, more easily linked to biologically active materials. Therefore, coccolith is considered to have broad application prospects in biomedical applications such as artificial bones, artificial teeth, and tissue engineering scaffold materials (Piattelli et al. 1997).

3.1.3 High value-added health products

Previous research found that *P. carterae* cells are rich in unsaturated fatty acids (ω-3 fatty acids) (Conte 1994). As a biologically active substance which is necessary for the human

body, omega-3 fatty acids play an important role in human growth and development. Among them, eicosapentaenoic acid (EPA) and docosahexaenoic acid (DHA) have special brain-enhancing effects (Nevenzel 1989).

The coccolith on the coccolithophore cell surface has high calcium content, small volume, and complex structure. It is easy to combine with human bioactive substances and improve the absorption and utilization rate of the human body. It can be used as a new type of calcium supplement (Nishimori and Morinaga 1996).

Also, coccolithophore cells are capable of enriching vitamin B_{12} and converting it to active VB_{12} or VB_{12}-containing coenzymes. Therefore, coccolithophore can be used as a nutrient to meet the body's demand for VB_{12} (Miyamoto et al. 2001).

3.1.4 Bioenergy

P. carterae can synthesize and accumulate oil in large quantities during the growth process and can be used to produce biofuels. The results of the Moheimani (Moheimani and Borowitzka 2006) study showed that the oil content of *P. carterae* reached 33% of the cell dry weight, and the outdoor culture study has shown that the biomass yield per unit area of the *P. carterae* in the run-to-cell reactor was 19.5 $g \cdot m^{-2} \cdot day^{-1}$. That is 60 $tons \cdot ha^{-1}$ annually yield of biomass and oil yield of 21.9 $tons \cdot ha^{-1} \cdot year^{-1}$.

4. Research objectives

The research on coccolithophore is currently focused on *Emiliania huxleyi* and there are relatively few studies on *Pleurochrysis carterae.*

Phosphorus participates in physiological activities such as signal transmission (b) energy conversion (c) photosynthesis it is one of the essential elements for the growth of

microalga. Different algae require different amounts of phosphorus.

Potassium is a variety of enzyme activator, plays an important role in metabolism: promote photosynthesis, promote nitrogen metabolism, improve plant nitrogen absorption. KNO_3 has not only potassium but also nitrogen; it is a very important nutrient for microalgae.

Most of the current experiments are for outdoor culture. There are few studies on the effect of phosphorus and KNO_3 concentration on the growth of *P. carterae* under artificial culture.

This study aimed to discover the effects of different nutrients on $CaCO_3$ and lipid content which are the two main products of *P. carterae*. The main research objectives are as following:

1) Effect of KNO_3 on various components of *P. carterae*
2) Effect of NaH_2PO_4 on various components of *P. carterae*
3) Further research on the structure of coccolith of *P. carterae*

5. References

Bell MV, Pond D. (1996). Lipid composition during growth of motile and coccolith forms of Emiliania huxleyi. Phytochemistry, 41:465-471

Benemann JR. (1997). CO_2 mitigation with microalgae systems. Energy Conversion and Management, 38:S475-S479

Blackburn S, Cresswell G. (1993). A coccolithophorid bloom in Jervis Bay. Australia Marine and Freshwater Research, 44:253-260

Borowitzka M. (1989). Carbonate calcification in algae-initiation and control Biomineralization. Chemical and Biochemical Perspectives:63-94

Borowitzka MA, Larkum A. (1987). Calcification in algae: mechanisms and the role of metabolism. Critical Reviews in Plant Sciences, 6:1-45

Brand, L. E. (2006). Physiological ecology of marine. Coccolithophores, 39.

Brownlee, C. (1994). Cellular regulation during calcification in Emiliania huxleyi. The Haptophyte Algae, 133-148.

Brownlee C, Taylor A. (2004). Calcification in coccolithophores: a cellular perspective. In: Coccolithophores. Springer, pp, 31-49

Buitenhuis ET, De Baar HJ, Veldhuis MJ. (1999). Photosynthesis and calcification by Emiliania huxleyi (Prymnesiophyceae) as a function of inorganic carbon species. Journal of Phycology, 35:949-959

Chilton FH, Rudel LL, Parks JS, Arm JP, Seeds MC. (2008). Mechanisms by which botanical lipids affect inflammatory disorders–. The American Journal of Clinical Nutrition, 87:498S-503S

Conte M. (1994). Lipid biomarkers of the Haptophyta. The Haptophyte Algae, 351-377

Cox PM, Betts RA, Jones CD, Spall SA, Totterdell IJ. (2000). Acceleration of global warming due to carbon-cycle feedbacks in a coupled climate model. Nature, 408:184

Daugbjerg N, Andersen RA. (1997). Phylogenetic analyses of the rbcL sequences from haptophytes and heterokont algae suggest their chloroplasts are unrelated. Molecular Biology and Evolution, 14:1242-1251

de Vrind-de Jong EW, de Vrind JP. (1997). Algal deposition of carbonates and silicates. Reviews in Mineralogy and Geochemistry, 35:267-307

Ehrlich HL. (1998). Geomicrobiology: its significance for geology. Earth-Science Reviews, 45:45-60

Galli L et al. (2014). Optimal dietary calcium intake in HIV treated patients: No femoral osteoporosis but higher cardiovascular risk. Clinical Nutrition, 33:363-366

Gao K, McKinley KR. (1994). Use of macroalgae for marine biomass production and CO2 remediation: a review. Journal of Applied Phycology, 6:45-60

Garcia de Acilu M, Leal S, Caralt B, Roca O, Sabater J, Masclans J. (2015). The role of omega-3 polyunsaturated fatty acids in the treatment of patients with acute respiratory distress syndrome: a clinical review. BioMed research international, 2015

Gattuso J-P, Buddemeier RW. (2000). Ocean biogeochemistry: calcification and CO2. Nature, 407:311

Geider RJ et al. (2001). Primary productivity of planet earth: biological determinants and

physical constraints in terrestrial and aquatic habitats. Global Change Biology, 7:849-882

Hase R, Oikawa H, Sasao C, Morita M, Watanabe Y. (2000). Photosynthetic production of microalgal biomass in a raceway system under greenhouse conditions in Sendai city. Journal of bioscience and bioengineering, 89:157-163

Hossain AS, Salleh A, Boyce AN, Chowdhury P, Naqiuddin M. (2008). Biodiesel fuel production from algae as renewable energy. American Journal of Biochemistry and Biotechnology 4:250-254

Houdan A, Bonnard A, Fresnel J, Fouchard S, Billard C, Probert I. (2004). Toxicity of coastal coccolithophores (Prymnesiophyceae, Haptophyta). Journal of Plankton Research, 26:875-883

Hulburt E. (1963). The diversity of phytoplanktonic populations in oceanic, coastal, and estuarine regions. Journal of Marine Research 21:81-93

Jeffrey S, Allen M. (1964). Pigments, Growth and Photosynthesis in Cultures of Two Chrysomonads, Coccolithus huxleyi and a Hymenomonassp. Microbiology, 36:277-288

Jensen GS. (2001). Blue-green algae as an immuno-enhancer and biomodulator. J Am Nutraceutical Assoc, 3:24-30

Jia Y-L, Xu W, Liu J-Q. (2004). Chemical Utilization of Carbon Dioxide Natural Gas Chemical Industry. C1 Chemistry and Technology, 3:012

Johansen JR, Doucette GJ, Barclay WR, Bull JD. (1988). The morphology and ecology of Pleurochrysis carterae var. dentata var. nov.(Prymnesiophyceae), a new

coccolithophorid from an inland saline pond in New Mexico, USA. Phycologia, 27:78-88

Keller MD. (1989). Dimethyl sulfide production in marine phytoplankton. Biogenic Sulfur In the Environment.

Klaveness D, Paasche E. (1971). Two different Coccolithus huxleyi cell types incapable of coccolith formation. Archiv für Mikrobiologie, 75:382-385

Le Quéré C et al. (2012). The global carbon budget 1959–2011. Earth System Science Data Discussions, 5:1107-1157

Leadbeater BS, Green J. (1994). The haptophyte algae. Systematics Association.

Malin G, Erst GO. (1997). Algal production of dimethyl sulfide and its atmospheric role 1. Journal of Phycology, 33:889-896

Marsh M. (1999). Coccolith crystals ofPleurochrysis carterae: Crystallographic faces, organization, and development. Protoplasma, 207:54-66

Marsh M. (2003). Regulation of CaCO3 formation in coccolithophores. Comparative Biochemistry and Physiology Part B: Biochemistry and Molecular Biology, 136:743-754

Marsh ME. (1994). Polyanion-mediated mineralization—assembly and reorganization of acidic polysaccharides in the Golgi system of a coccolithophorid alga during mineral deposition. Protoplasma, 177:108-122

McIntyre A. (1967). Coccoliths as paleoclimatic indicators of Pleistocene glaciation. Science, 158:1314-1317

Meisen A, Shuai X. (1997). Research and development issues in CO2 capture. Energy

Conversion and Management, 38:S37-S42

Metz, B., Davidson, O., & De Coninck, H. (Eds.). (2005). Carbon dioxide capture and storage: special report of the intergovernmental panel on climate change. Cambridge University Press.

Meyer A et al. (2004). Novel fatty acid elongases and their use for the reconstitution of docosahexaenoic acid biosynthesis. Journal of Lipid Research, 45:1899-1909

Miyamoto E et al. (2001). Characterization of a vitamin B12 compound from unicellular coccolithophorid alga (Pleurochrysis carterae). Journal of Agricultural and Food Chemistry, 49:3486-3489

Moheimani NR. (2005). The culture of coccolithophorid algae for carbon dioxide bioremediation. Murdoch University

Moheimani NR, Borowitzka MA. (2006). The long-term culture of the coccolithophore Pleurochrysis carterae (Haptophyta) in outdoor raceway ponds. Journal of Applied Phycology, 18:703-712

Nevenzel JC. (1989). Biogenic hydrocarbons of marine organisms. Marine Biogenic Lipids, Fats, and Oils, 1:3-72

Nimer N, Merrett M. (1993). Calcification rate in Emiliania huxleyi Lohmann in response to light, nitrate and availability of inorganic carbon. New Phytologist, 123:673-677

Nishimori T, Morinaga T. (1996). Safety evaluation of Pleurochrysis carterae as a potential food supplement. J Mar Biotechnol, 3:274-277

Ohsumi T. (2004). Introduction: what is the ocean sequestration of carbon dioxide?

Journal of Oceanography, 60:693-694

Outka D, Williams D. (1971). Sequential coccolith morphogenesis in Hymenomonas carterae. The Journal of Protozoology, 18:285-297

Paasche E. (1964). A tracer study of the inorganic carbon uptake during coccolith formation and photosynthesis in the coccolithophorid Coccolithus huxleyi. Physiol Plant Suppl, 3:1-82

Paasche E. (1967). Marine plankton algae grown with light-dark cycles. I. Coccolithus huxleyi. Physiologia Plantarum, 20:946-956

Paasche E. (1968). Biology and physiology of coccolithophorids. Annual Reviews in Microbiology, 22:71-86

Paasche E. (1998). Roles of nitrogen and phosphorus in coccolith formation in Emiliania huxleyi (Prymnesiophyceae). European Journal of Phycology, 33:33-42

Paasche E. (2001). A review of the coccolithophorid Emiliania huxleyi (Prymnesiophyceae), with particular reference to growth, coccolith formation, and calcification-photosynthesis interactions. Phycologia, 40:503-529

Packer M. (2009). Algal capture of carbon dioxide; biomass generation as a tool for greenhouse gas mitigation with reference to New Zealand energy strategy and policy. Energy Policy, 37:3428-3437

Piattelli A, Podda G, Scarano A. (1997). Clinical and histological results in alveolar ridge enlargement using coralline calcium carbonate. Biomaterials, 18:623-627

Pulz O, Gross W. (2004). Valuable products from biotechnology of microalgae. Applied Microbiology and Biotechnology, 65:635-648

Raven JA. (1997). Putting the C in phycology. European Journal of Phycology, 32:319-333

Reginster J-YL. (1995). Treatment of bone in elderly subjects: calcium, vitamin D, fluor, bisphosphonates, calcitonin. Hormone Research in Paediatrics, 43:83-88

Rodolfi L, Chini Zittelli G, Bassi N, Padovani G, Biondi N, Bonini G, Tredici MR. (2009). Microalgae for oil: Strain selection, induction of lipid synthesis and outdoor mass cultivation in a low-cost photobioreactor. Biotechnology and Bioengineering, 102:100-112

Rost B, Riebesell U. (2004). Coccolithophores and the biological pump: responses to environmental changes. In: Coccolithophores. Springer, pp 99-125

Schenk PM et al. (2008). Second generation biofuels: high-efficiency microalgae for biodiesel production. Bioenergy research, 1:20-43

Schröder R et al. (2012). PGH1, the precursor for the anti-inflammatory prostaglandins of the 1-series, is a potent activator of the pro-inflammatory receptor CRTH2/DP2. PloS one, 7:e33329

Shiraiwa Y. (2003). Physiological regulation of carbon fixation in the photosynthesis and calcification of coccolithophorids. Comparative Biochemistry and Physiology Part B: Biochemistry and Molecular Biology, 136:775-783

Sieburth JM. (1960). Acrylic acid, an" antibiotic" principle in Phaeocystis blooms in Antarctic waters. Science, 132:676-677

Sikes CS, Roer RD, Wilbur KM. (1980). Photosynthesis and coccolith formation: inorganic carbon sources and net inorganic reaction of deposition. Limnology and

Oceanography, 25:248-261

Sikes CS, Wilbur KM. (1980). Calcification by coccolithophorids: effects of pH and sr 1. Journal of Phycology, 16:433-436

Simopoulos AP. (2002). Omega-3 fatty acids in inflammation and autoimmune diseases. Journal of the American College of Nutrition, 21:495-505

Spolaore P, Joannis-Cassan C, Duran E, Isambert A. (2006). Commercial applications of microalgae. Journal of Bioscience and Bioengineering. 101:87-96

Surette ME, Edens M, Chilton FH, Tramposch KM. (2004). Dietary echium oil increases plasma and neutrophil long-chain (n-3) fatty acids and lowers serum triacylglycerols in hypertriglyceridemic humans. The Journal of nutrition, 134:1406-1411

Sverdrup LE, Källqvist T, Kelley AE, Fürst CS, Hagen SB. (2001). Comparative toxicity of acrylic acid to marine and freshwater microalgae and the significance for environmental effects assessments. Chemosphere, 45:653-658

Tyrrell T, Holligan P, Mobley C. (1999). Optical impacts of oceanic coccolithophore blooms. Journal of Geophysical Research: Oceans, 104:3223-3241

Van Alstyne KL, Houser LT. (2003). Dimethylsulfide release during macroinvertebrate grazing and its role as an activated chemical defense. Marine Ecology Progress Series, 250:175-181

Van der Wal P, De Jong L, Westbroek P, De Bruijn W. (1983). Calcification in the coccolithophorid alga Hymenomonas carterae. Ecological Bulletins, 251-258

Wadolowska L, Sobas K, Szczepanska JW, Slowinska MA, Czlapka-Matyasik M,

Niedzwiedzka E. (2013). Dairy products, dietary calcium and bone health: possibility of prevention of osteoporosis in women: the Polish experience. Nutrients, 5:2684-2707

Wen Z-Y, Chen F. (2003). Heterotrophic production of eicosapentaenoic acid by microalgae. Biotechnology Advances, 21:273-294

Wu YH, Yu Y, Hu HY. (2013). Potential biomass yield per phosphorus and lipid accumulation property of seven microalgal species. Bioresource technology, 130:599-602

Young JR, Bown PR. (1991). An ontogenic sequence of coccoliths from the Late Jurassic Kimmeridge Clay of England. Palaeontology, 34:843-850

Zhou CX, Yan XJ, Sun X, Xu JL, Fu YJ. (2008). The experimental observations and characteristics of one strain of coccolithophorid from the bloom water in a shrimp pool, ZheJiang, China. Acta Hydrobiologica Sinica, 6:025

CHAPTER II

The effect of NaH_2PO_4 on $CaCO_3$ accumulation and lipids synthesis of *Pleurochrysis carterae*

Xuantong Chen[1, 2], Fan Lu[3*], Wensheng Qin[1*]

[1]Department of Biology, Lakehead University, 955 Oliver Road, Thunder Bay, Ontario, P7B 5E1, Canada.

[2]Faculty of Natural Resources Management, Lakehead University, 955 Oliver Road, Thunder Bay, Ontario, P7B 5E1, Canada.

[3]School of Civil Engineering, Architecture and Environment, Hubei University of Technology, Wuhan, 430068, China.

* Corresponding authors: wqin@lakeheadu.ca, lf1230nc@yahoo.com

Abstract

Pleurochrysis carterae is a marine microalga with various potential applications. *P. carterae* was cultured in f/2 media with four different concentrations of NaH_2PO_4. After a long period of culturing time, the optimal NaH_2PO_4 concentration for inducing *P. carterae* proliferation was 1.5 mM; if the culture time was less than 15 days, the optimal NaH_2PO_4 concentration for inducing *P. carterae* proliferation was 0.05 mM. When the concentration of NaH_2PO_4 was higher than 0.5 Mm, it could decrease the pH value of the culture medium in the first few days and it has the lowest pH value at 6.21 with 2 mM of NaH_2PO_4 on day 2 and it which was presumed that *P. carterae* is synthesizing an acidic substance. The highest $CaCO_3$ content was 7.26 % of the algal dry weight in the medium with a NaH_2PO_4 concentration of 0.5 mM and the calcification of the *P. carterae* was

inhibited under 1.5 mM and 2.0 mM concentration of NaH_2PO_4. Moreover, within the tested range, the concentration of NaH_2PO_4 is negatively related to the accumulation of lipids in *P. carterae*. Experiments have also confirmed that NaH_2PO_4 promotes the synthesis of more chlorophyll α in *P. carterae,* In 2 mM concentration of NaH_2PO_4 medium, the chlorophyll α content can reach 6.37 $mg \cdot L^{-1}$.

Keywords: *Pleurochrysis carterae*, Calcium, Lipid, pH, chlorophyll

1. Introduction

Pleurochrysis carterae is a marine microalga also known as coccolithophorid (Paasche 1968). Like most photosynthetic organisms, *P. carterae* can synthesize organic materials such as lipids, carbohydrates, protein through photosynthesis. *P. carterae* can fix carbon dioxide and HCO_3^- by photosynthesis and its special calcification (Marsh 2003). Moreover, its cells are rich in lipids, and its lipid content can account for 33% of dry weight (Moheimani and Borowitzka 2006), of which the long-chain unsaturated fatty acids DHA (22:6ω-3, docosahexaenoic acid) accounts for 30% ~40% of total lipid content (Bell and Pond 1996).

Phosphorus is one of the essential elements for the growth of microalga (Wu et al. 2013). Commonly used phosphorus sources are phosphate and hydrogen phosphate. Phosphorus plays an important role in the metabolic process of algae cells and aquatic ecosystems (Larned 1998). It participates in physiological activities such as signal transmission, energy conversion and photosynthesis, and it is one of the reasons why phytoplankton competes to produce dominant populations in water. Phosphorus in algae cells usually accounts for 1% of the dry weight of cells (Borchardt and Azad 1968). However, due to the formation of complexes with metal ions, not all added phosphates are bioavailable. Therefore, it may be required that large amounts of phosphate add into the water for the efficiency of the application of algae (Chisti 2007).

Different algae require different amounts of phosphorus. Previous studies have found that the optimal phosphorus concentration required for the growth of *Chlorella zofingiensis* is 0.044 $mmol \cdot L^{-1}$ (Feng et al. 2012). However, the optimal phosphorus concentration

required for *Dunaliella salina* growth is 11.7 mmol·L^{-1} (Hanhua Chen 1997). Too low or too high concentration of phosphorus could inhibit cell growth (Grobbelaar 2003).

Previous studies have suggested that phosphorus deficiency induces calcification of coccolithophore *Emiliania huxleyi*, forming coccolith, and also induces cell enlargement (Paasche 1998; Riegman et al. 2000). It has also been found that the blooming of coccolithophore *E. huxleyi* occurs in the areas with low nitrogen and high phosphorus concentrations (Balch et al. 1991; Tyrrell and Merico 2004; Ziveri et al. 1995).

At present, the data on the effect of phosphorus concentration on the growth of coccolithophore mostly come from the study of marine ecology. Due to the complexity of marine ecosystems, the factors affecting the growth of coccolithophore are not clear, so the previous results cannot objectively reflect the algae situation in artificial culture. There are few studies on the effect of phosphorus concentration on the growth of coccolithophore *P. carterae* under artificial culture. Therefore, this article will use several different concentrations of NaH_2PO_4 to culture coccolithophore *P. carterae* and measure the content of each component, laying the foundation for subsequent research. Based on the previous study on coccolithophore *E. huxleyi*, we propose that high concentration of NaH_2PO_4 could inhibit the $CaCO_3$ and lipid accumulation in *P. carterae.*

2. Materials and methods

2.1. Algal strain

Pleurochrysis carterae was purchased from National Center for Marine Algae and Microbiota (NCMA - https://ncma.bigelow.org/ccmp646) (Kindly provided by Dr. Fan Lu, Hubei University of Technology, China).

2.2. Preparation of f/2 medium

The f/2 medium (pH 8.0) contain 225 mg·L^{-1} $NaNO_3$, 5.6 mg·L^{-1} $NaH_2PO_4·H_2O$, 1 ml·L^{-1} trace metal solution, and 0.5 ml·L^{-1} vitamin solution. The trace metal solution is composed of 315 mg $FeCl_3·6H_2O$, 436 mg $Na_2EDTA·2H_2O$, 9.8 mg $CuSO_4·5H_2O$, 6.3 mg $Na_2NoO_4·2H_2O$, 22 mg ZnSO4·$7H_2O$, 10 mg $CoCl_2·6H_2O$, and 180 mg $MnCl_2·4H_2O$ dissolved in a final volume of 100 ml distilled water. The vitamin solution is composed of 20 mg thiamine HCl (vitamin B_1), 10 mg biotin (vitamin H), and 10 mg cyanocobalamin (vitamin B_{12}) dissolved in a final volume of 100 ml distilled water.

2.3. Algal culturing

P. carterae were cultured in f/2 medium (Guillard and Ryther 1962) with different concentrations of NaH_2PO_4 (0.05, 0.5, 1.5, 2 mM) and 0.05 mM as control and each concentration have three replicates. The starting cell density was $1.5×10^5$ cells per liter. The culture temperature was set at 26°C with 16/8 hours light and dark photocycle provided by cold white fluorescent light and 24 hours continuous air pumping.

2.4. Sample collection

For calcium and lipid content measurement, 200 ml *P. carterae* cells were collected by centrifugation at 5,000 r·min^{-1} for 10 minutes at days 0, 10, 15, 20, 25, 30. The pellets were washed twice with distilled water, and the samples were oven dried at 105 ℃ until the weight remained stable.

2.5. *P. carterae* calcium content measurement

2.5.1. Sample decolorization

The samples were decolorized with 75 % ethanol before measuring the calcium content

(Corstjens and Gonzalez 2004; Daugbjerg and Andersen 1997; Dyhrman et al. 2006). 1 ml of ethanol was added into 0.01 mg of the dry algae. After 30 minutes of the water bath (80℃), the samples were collected by centrifugation at 12,000 $r \cdot min^{-1}$ for 30 minutes. The supernatant was then discarded, and the steps were repeated until the supernatant was colorless.

2.5.2. Calcium content measurement of decolorization samples

Decolorized samples were mixed with 1.5 ml of 2 N HCl followed by a water bath (80 ℃) for 30 minutes to remove CO_2. The supernatant containing $CaCl_2$ was collected by centrifugation at 12,000 $r \cdot min^{-1}$ for 3 minutes. The calcium ion content in the supernatant was measured by the ethylenediaminetetraacetic acid (EDTA) complexometric titration method (Wang et al. 2007). The end-point was recorded and determined by observing when the color of the calconcarboxylic acid (Calcon indicator) changed from red to blue and remained for at least 30 seconds.

Calcium ion content ($mg \cdot L^{-1}$) was calculated according to the following Equation 1:

$$\mathrm{Ca} = \frac{\mathrm{M} \times \mathrm{a} \times 40.08}{\mathrm{V}} \times 1000 \qquad \text{Equation 1}$$

M: EDTA standard solution molar concentration

a: The volume (ml) of EDTA standard solution being consumed during the titration

V: Sample volume (ml)

The atomic weight of calcium: 40.08

The calcium ion content in the sample is calculated based on the standard curve.

2.6. Total lipid measurement

Lipids were extracted using the chloroform-methanol extraction method (Bligh and Dyer

1959). Dry algae powder of 0.01 g was transferred to a 1.5 ml centrifuge tube. Then, 395 µl chloroform, 790 µl methanol, and 316 µl deionized water were added, to make a ratio of 1: 2: 0.8 (V: V: V). This was then mixed by vortex for 3 to 5 minutes, followed by 3 minutes of centrifugation at 12,000 r·min^{-1}. The supernatant was collected in a glass tube, and the above operation was repeated three more times.

Once all supernatant was collected in a 15 ml glass tube, chloroform, methanol, and water were added to make the final volume ratio 1: 1: 0.9 (V: V: V). The solution was mixed well and left until complete phase separation occurred. The bottom layer was then collected to a pre-weighed tube, recorded as M1 (g), and placed in the fume hood overnight. The tube was further dried in the oven at 105 ℃ until the weight was constant, then weighed and recorded as M2 (g). The lipid content was calculated according to following Equation 2:

$$\text{Lipids content (\%)} = \frac{\text{M2 (g)} - \text{M1(g)}}{\text{0.01 (g)}} \times 100\% \qquad \text{Equation 2}$$

2.7. Chlorophyll α determination

The methanol extraction method was used for chlorophyll α determination (Chen et al. 2008). The pellet collected from the centrifugation (12, 000 r·min^{-1} for 2-3 minutes) of algae fluid (200 µl) was mixed with methanol (800 µl) and shaken in a 60 ℃ water bath for 15 minutes. After that, the mixture was placed in the dark and cooled for 30 minutes, then centrifuged again (12, 000 r·min^{-1} for 2-3 minutes). The supernatant was moved to a 2 ml centrifugation tube, then volume to 1 ml with methanol. The above steps were then replaced again. Optical density was measured at 665 and 750 nm. Chlorophyll α concentration was determined by following Equation 3:

$$\text{Chlorophylla } \alpha\ (\text{mg} \cdot \text{L}^{-1}) = 13.9 \times (\text{OD}_{665} - \text{OD}_{750}) \times \frac{U\ (L)}{V\ (L)} \qquad \text{Equation 3}$$

U: final methanol volume

V: sample volume

3. Results

3.1. The effect of NaH_2PO_4 on cell number of *P. carterae*

In this experiment, we conducted a 30-day measurement on *P. carterae*' s cell number, pH value of the medium, $CaCO_3$ content, lipid content and chlorophyll α content, respectively. The changes in *P. carterae* cell numbers in 30 days are shown in Fig. 1. From the results of day 0 to day 14, the number of algal cells is inversely related to the concentration of NaH_2PO_4. From day 16 to day 22, the amount of *P. carterae* cells grown in 0.5, 1.5 and 2 mM NaH_2PO_4 medium increased rapidly and exceeded the number of cells in the control group on day 16. The number of cells in the four groups reached the maximum on day 22. Among them, under 1.5 mM of NaH_2PO_4, *P. carterae* has the largest cell population of $32.67 \times 10^5 \cdot ml^{-1}$. From the day 22 to the day 30, the population of algae cells in the four groups of culture medium began to decrease, and the order of the number of cells in the four concentrations of NaH_2PO_4 medium was 1.5 mM > 2.0 mM > 0.5 mM > control.

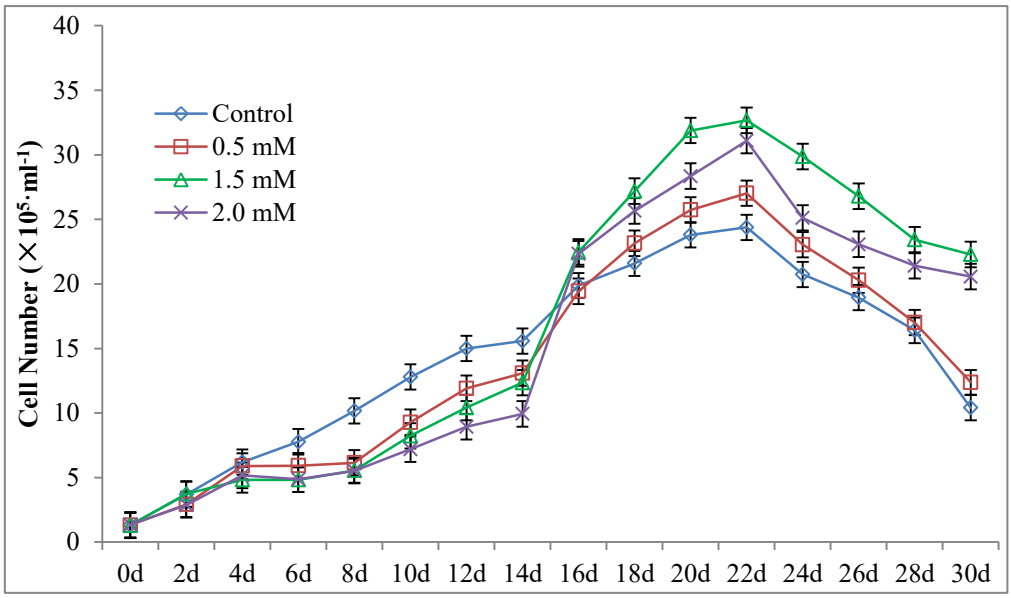

Fig. 1 30 days' cell number trend of *P. carterae* growing in f/2 medium containing different concentrations of NaH_2PO_4 (0.05 mM as control, 0.5, 1.5 and 2 mM)

3.2. The effect of NaH_2PO_4 on pH changes in algal medium

P. carterae could bloom in a suitable environment (Moheimani and Borowitzka 2006) and during the growth of *P. carterae*, dimethylsulfide (DMS) is produced, which can acidify the ocean (Stefels 2000). In this research, the pH changes of the culture medium during the growth of *P. carterae* under different concentrations of NaH_2PO_4 were investigated (Fig.2). Under 0.05 mM of NaH_2PO_4, the pH in the medium has almost no change within 30 days. When the NaH_2PO_4 concentration is 0.5 mM, the pH in the medium decreased from 8 to 7, from day 0 to day 10. After that, from day 10 to day 30, the pH in the medium slowly increased from pH 7 to 7.6. Interestingly, in group 1.5 mM and 2 mM, the pH in the medium dropped dramatically from pH 8 to 6.5 on day 2, respectively. In the 1.5 mM concentration of NaH_2PO_4 medium, the pH value increased from 6.5 to 7.7, from day 2 to day 16, after that the pH value became stable from day 16 to day 30, maintained the pH at around 7.7. In the medium with a NaH_2PO_4 concentration

of 2 mM, the pH rose sharply from 6.2 to 7.9, from day 2 to day 14. After this, the pH value tends to be stable, and the highest pH value appears on day 26, and its pH is 8.2.

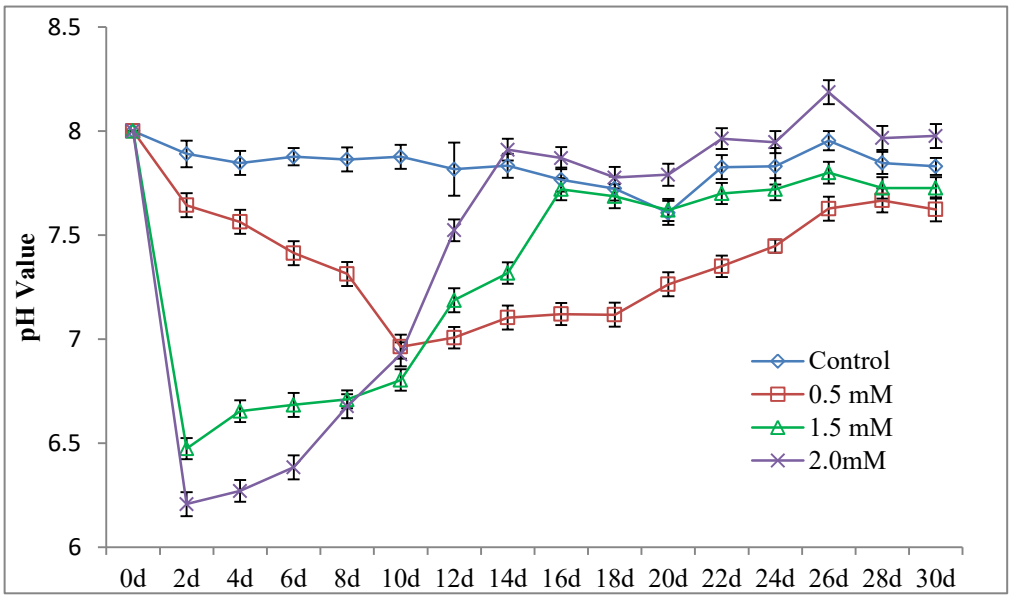

Fig. 2 30 days' pH changes trend in algal medium containing different concentrations of NaH_2PO_4 (0.05 mM as control, 0.5, 1.5 and 2 mM)

3.3. The effect of NaH_2PO_4 on $CaCO_3$ accumulation of *P. carterae*

Previous studies have found that when the NaH_2PO_4 is deficient in coccolithophore *E. huxleyi*, it promotes the synthesis of calcium carbonate (Paasche 1998; Riegman et al. 2000). However, little research has been done on the effects of NaH_2PO_4 on *P. carterae* calcification. Figure 3 shows the trend of calcium content of *P. carterae* in different concentrations (0.05 mM as control, 0.5, 1.5 and 2 mM) of NaH_2PO_4 as culture conditions. The calcium content of the 0.5mM group increased from 5.32 % on day 0 to 7.26 % on day 10, and then gradually descended from the day 10 to the day 30, when calcium content was 5.82 %. In the control group, the calcium content of *P. carterae* slowly increased from 5.32 % on day 0 to 6.44 % on day 10, and then gradually decreased to 4.5 % on day 30. However, the overall trend of 30-day calcium content in the medium

with a concentration of 1.5 mM and 2 mM showed a downward trend from 5.32 % on day 0 to 4.12 % and 3.0 % on the day 30, respectively.

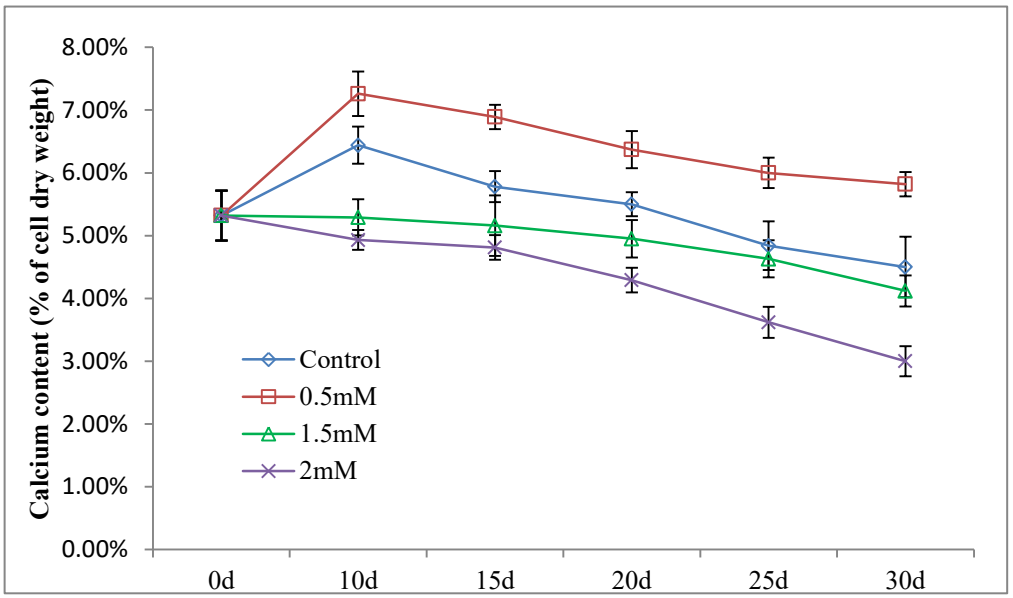

Fig. 3 30 days' calcium content trend of *P. carterae* growing in f/2 medium containing different concentrations of NaH_2PO_4 (0.05 mM as control, 0.5, 1.5 and 2 mM)

3.4. The effect of NaH_2PO_4 on lipid accumulation of *P. carterae*

Figure 4 shows the trend of lipid accumulation in *P. carterae* grown in different concentrations of NaH_2PO_4 within 30 days. From day 0 to day 20, the lipid content of *P. carterae* cultured under the four NaH_2PO_4 concentrations showed a downward trend. The initial lipid concentrations of the four groups of samples were approximately 33 %. The lipid content dramatically decreased from 33.7 % to 5 % in the medium containing 2 mM of NaH_2PO_4. The lowest rate of decrease in lipid content was in the control group, which decreased from 33.1 % to 20.5 %. The lipid content of the other two groups also decreased, with a decrease of 26.4 % in the 0.5 mM group and a 27 % decrease in the 1.5 mM group. Interestingly, the lipid content of the four groups began to rise after day 20 until day 30 in the order of control, 0.5 mM, 1.5 mM, 2 mM, the lipid content increased

by 7.2 %, 15.3 %, 8.5 %, and 5.5 %， respectively, from the day 20 to day30.

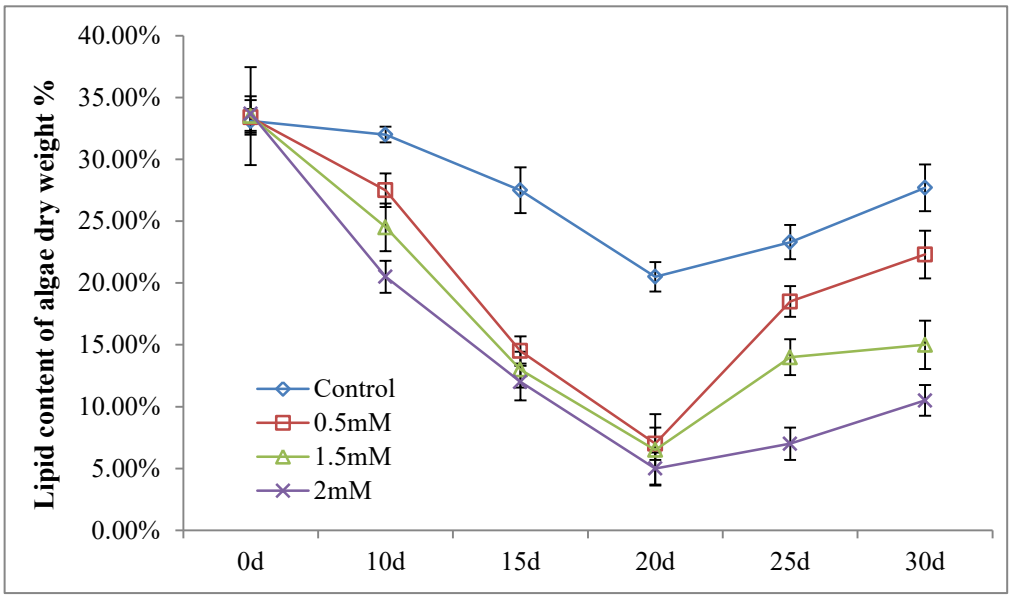

Fig. 4 30 days' lipid accumulation trend of *P. carterae* growing in f/2 medium containing different concentrations of NaH_2PO_4 (0.05 mM as control, 0.5, 1.5 and 2 mM)

3.5. The effect of NaH_2PO_4 on chlorophyll α content of *P. carterae*

Figure 5 shows the trend of chlorophyll α content in *P. carterae*'s medium with different NaH_2PO_4 content within 30 days. The content of chlorophyll α in *P. carterae* was much higher than that in the other three groups when NaH_2PO_4 concentration is 2 mM, and the highest chlorophyll α content was on day 26 at 6.37 $mg \cdot L^{-1}$. Under 1.5 mM of NaH_2PO_4, the highest chlorophyll α content of the *P. carterae* was 4.47 $mg \cdot L^{-1}$, on day 30. The highest content of chlorophyll α in the medium with 0.5 mM of NaH_2PO_4 was 3.13 $mg \cdot L^{-1}$, on day 26. The chlorophyll α content of the control group did not change much, only increased by 1.03 $mg \cdot L^{-1}$, from day 0 (0.49 $mg \cdot L^{-1}$) to day 28 (1.52 $mg \cdot L^{-1}$).

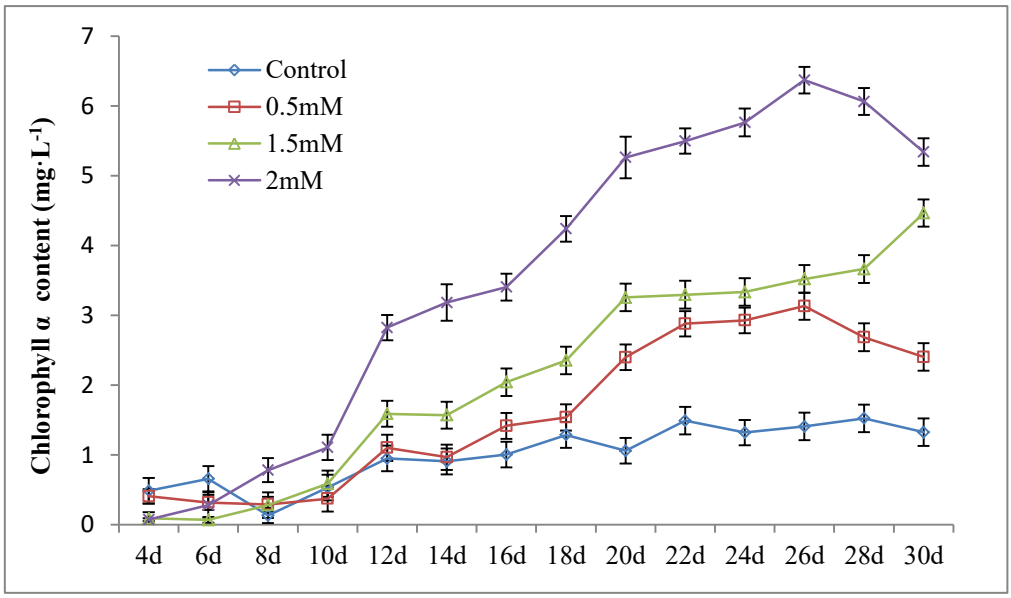

Fig. 5 30 days' chlorophyll α trend of *P. carterae* growing in f/2 medium containing different concentrations of NaH_2PO_4 (0.05 mM as control, 0.5, 1.5 and 2 mM)

4. Discussion

In this research, the effects of four concentrations of NaH_2PO_4 (0.05 mM as control, 0.5, 1.5 and 2 mM) on cell population, pH changes of culture medium, $CaCO_3$ content, lipid content and chlorophyll α content in *P. carterae* were studied. From the results of the cell population (Fig. 1), it can be determined that the culture period of *P. carterae* is 22 days, and the number of cells in the four groups reached the maximum on the day 22. This demonstrates that changes in the concentration of NaH_2PO_4 in the medium do not affect the cultural period of the *P. carterae*, but affect the number of cells in the *P. carterae*. Moreover, under long-term culture conditions, *P. carterae* has the largest cell numbers on day 22 when the NaH_2PO_4 concentration is 1.5 mM, but if the culture days are less than 14 days, it is a larger cell number occurred in the control group (0.05 mM). The reason for this phenomenon can be seen by comparing Figure 1 and Figure 2; the addition of NaH_2PO_4 induces the *P. carterae* to synthesize an acidic substance which decreases the

pH in the medium, which is not conducive to the proliferation of the *P. carterae* cells. In terms of dosage, 1.5 mM of NaH_2PO_4 30 times more than 0.05 mM of NaH_2PO_4. By considering an economic point of view, the 0.05 mM NaH_2PO_4 solution is more cost effective.

The change of pH in the medium within 30 days (Fig. 2), we can see that 0.5, 1.5 and 2.0 mM of NaH_2PO_4 induces *P. carterae* to release acidic substances in the early growth stage. We speculate that the more phosphorus could induce *P. carterae* to synthesize dimethylsulfide (DMS) when compared to the control. In the three concentrations of NaH_2PO_4 (0.5, 1.5 and 2 mM), the pH value in the medium and the amount of NaH_2PO_4 added showed a negative correlation. That is, from day 0 to day 2, the higher NaH_2PO_4 content could result in the lower of the pH of the medium.

Previous studies have found that low concentrations of phosphorus can induce calcification of coccolithophore *E. huxleyi* (Paasche 1998). From the result, it can be seen that with the NaH_2PO_4 concentration of 0.05 mM or 0.5 mM, the amount of the calcium accumulation of *P. carterae* gradually increased from day 0 to day 10. However, under 1.5 mM or 2 mM phosphorus concentration, the trend of calcium accumulation was decreased gradually from day 0 to day 30. We speculate that 1.5 mM and 2.0 mM concentrations of NaH_2PO_4 inhibit the calcification process of *P. carterae* cells, and if the NaH_2PO_4 concentration is 0.5 Mm or without NaH_2PO_4, it induces calcification of *P. carterae* cells. This result is similar to that in coccolithophore *E. huxleyi* (Balch et al. 1991; Tyrrell and Merico 2004; Ziveri et al. 1995).

When the NaH_2PO_4 in the medium is relatively low (Fig. 4), the intracellular lipid content

could be relatively high. Medium containing 0.5, 1.5, 2.0 Mm of NaH_2PO_4 inhibits the lipids synthesis in *P. carterae* cells. By combining with Figure 1, it can be seen that when the *P. carterae* cells are active, the intracellular lipid content decreases from day 0 to day 20. From day 20 to day 30, the cells begin to enter the senescence phase, and even enter the dormant phase, thus, lipid content in the *P. carterae* cells begins to increase, but it can be seen that 0.5, 1.5, 2.0 Mm of NaH_2PO_4 still inhibit the synthesis of intracellular lipids. We observed that with the increase of NaH_2PO_4 concentration, the content of chlorophyll α was increased (Fig. 5). This result suggests that NaH_2PO_4 can promote the synthesis of chlorophyll α in *P. carterae*. In this experiment, *P. carterae* can synthesize more chlorophyll α when the NaH_2PO_4 concentration is 2 mM. Further experiments are needed for optimizing the best concentration of NaH_2PO_4 for chlorophyll α synthesis. Through this experiment, we can conclude that during the cultivation of *P. carterae*, 0.5, 1.5, 2.0 mM of NaH_2PO_4 induces the cells to secrete acidic substances in the early stage to lower the pH of the medium and reduce the intracellular lipids synthesis, and 1.5, 2.0 mM of NaH_2PO_4 inhibit the synthesis of $CaCO_3$. However, 0.5, 1.5, 2.0 mM of NaH_2PO_4 can accelerate the proliferation of cells and enhance the content of chlorophyll α content.

5. References

Balch WM, Holligan PM, Ackleson SG, Voss KJ. (1991). Biological and optical properties of mesoscale coccolithophore blooms in the Gulf of Maine. Limnology and Oceanography, 36:629-643

Bell MV, Pond D. (1996). Lipid composition during growth of motile and coccolith forms of Emiliania huxleyi. Phytochemistry, 41:465-471

Bligh EG, Dyer WJ. (1959). A rapid method of total lipid extraction and purification. Canadian Journal of Biochemistry and Physiology, 37:911-917

Borchardt JA, Azad HS. (1968). Biological extraction of nutrients. Journal (Water Pollution Control Federation), 1739-1754

Chen GW, Choi SJ, Lee TH, Lee GY, Cha JH, Kim CW. (2008). Application of biocathode in microbial fuel cells: cell performance and microbial community. Applied Microbiology and Biotechnology, 79:379-388

Chisti Y. (2007). Biodiesel from microalgae. Biotechnology advances, 25:294-306

Corstjens PL, Gonzalez EL. (2004). Effects of nitrogen and phosphorus availability on the expression of the coccolith-vesicle V-ATPase (subunit c) of Pleurochrysis (Haptophyta). Journal of Phycology, 40:82-87

Daugbjerg N, Andersen RA. (1997). Phylogenetic analyses of the rbcL sequences from haptophytes and heterokont algae suggest their chloroplasts are unrelated. Molecular Biology and Evolution, 14:1242-1251

Dyhrman ST, Haley ST, Birkeland SR, Wurch LL, Cipriano MJ, McArthur AG. (2006). Long serial analysis of gene expression for gene discovery and transcriptome

profiling in the widespread marine coccolithophore Emiliania huxleyi. Applied and Environmental Microbiology, 72:252-260

Feng P, Deng Z, Fan L, Hu Z. (2012). Lipid accumulation and growth characteristics of Chlorella zofingiensis under different nitrate and phosphate concentrations. Journal of Bioscience and Bioengineering, 114:405-10.

Grobbelaar JU. (2003). Algal Nutrition–Mineral Nutrition. Handbook of Microalgal Culture: Biotechnology and Applied Phycology, 95-115.

Guillard RR, Ryther JH. (1962). Studies of marine planktonic diatoms: I. Cyclotella nana Hustedt, and Detonula confervacea (Cleve) Gran. Canadian journal of microbiology, 8:229-239

Hanhua Chen, K. Q. (1997). Effects of Nitrogen and Phosphorus on the Growth and β-Carotene Accumulation of Dunaliella Salina. Journal of Zhejiang University (Natural Science Edition), 31(6):7 31-736.

Larned S. (1998). Nitrogen-versus phosphorus-limited growth and sources of nutrients for coral reef macroalgae. Marine Biology, 132:409-21.

Marsh M. (2003). Regulation of CaCO3 formation in coccolithophores. Comparative Biochemistry and Physiology Part B: Biochemistry and Molecular Biology, 136:743-754

Moheimani NR, Borowitzka MA. (2006). The long-term culture of the coccolithophore Pleurochrysis carterae (Haptophyta) in outdoor raceway ponds. Journal of Applied Phycology, 18:703-712

Paasche E. (1968). Biology and physiology of coccolithophorids. Annual Reviews in

Microbiology, **22**:71-86.

Paasche E. (1998). Roles of nitrogen and phosphorus in coccolith formation in Emiliania huxleyi (Prymnesiophyceae). European Journal of Phycology, 33:33-42

Riegman R, Stolte W, Noordeloos AA, Slezak D. (2000). Nutrient uptake and alkaline phosphatase (EC 3: 1: 3: 1) activity of Emiliania huxleyi (Prymnesiophyceae) during growth under N and P limitation in continuous cultures. Journal of Phycology, 36:87-96

Stefels J. (2000). Physiological aspects of the production and conversion of DMSP in marine algae and higher plants. Journal of Sea Research, 43:183-197

Tyrrell T, Merico A. (2004). Emiliania huxleyi: bloom observations and the conditions that induce them. In: Coccolithophores. Springer, pp 75-97

Wang ZF, Song BC, Zhang J. (2007). Precise Measurement of Ca and P Content in Hydroxyapatite by Chemical Analysis [J]. Bulletin of the Chinese Cerrmic Society, 1:040

Wu YH, Yu Y, Hu HY. (2013). Potential biomass yield per phosphorus and lipid accumulation property of seven microalgal species. Bioresource technology, 130:599-602

Ziveri P, Thunell R, Rio D. (1995). Seasonal changes in coccolithophore densities in the Southern California Bight during 1991–1992. Deep Sea Research Part I: Oceanographic Research Papers, 42:1881-903.

CHAPTER III

Effect of KNO_3 on Lipid Synthesis in *Pleurochrysis carterae* and $CaCO_3$ Accumulation in Its Shells

Xuantong Chen[1, 2], Fan Lu[3*], Wensheng Qin[1*]

[1]Department of Biology, Lakehead University, 955 Oliver Road, Thunder Bay, Ontario, P7B 5E1, Canada.

[2]Faculty of Natural Resources Management, Lakehead University, 955 Oliver Road, Thunder Bay, Ontario, P7B 5E1, Canada.

[3]School of Civil Engineering, Architecture and Environment, Hubei University of Technology, Wuhan, 430068, China.

* Corresponding authors: wqin@lakeheadu.ca, lf1230nc@yahoo.com

Abstract

Pleurochrysis carterae is a marine alga found in oceans that affect the carbon cycle in the environment. *P. carterae* were cultured in f/2 media with various concentrations of KNO_3 (0.25, 0.5, 0.75, one mmol·L^{-1}, without KNO_3 is used as a control). The results of complexometric titration and Scanning Electron Microscope (SEM) showed that $CaCO_3$ was highly accumulated on the surface of the algae, and the cell size of *P. carterae* reached the maximum under 0.75 mmol·L^{-1} of KNO_3. During 10 days of culture, the content of lipids and carbohydrate both decreased, but protein content slightly increased. The FTIR results are consistent with the increase of protein and decrease of lipids and carbohydrate. With 1 mmol·L^{-1} of KNO_3 in the medium, the *P. carterae* had the lowest amount of carbohydrate at 21.08 % of dry algal weight and the highest amount of proteins at 32.87 % of dry algal weight on day 10. The highest yield of lipids in *P.*

carterae reached 33.61 % of its dry-biomass in control on day 10, and when the KNO_3 concentration was 1 $mmol \cdot L^{-1}$, it reached the lowest lipid content which was only 13.67 %. However, medium with higher than 1 $mmol \cdot L^{-1}$of KNO_3 could inhibit the cell size of *P. carterae* and $CaCO_3$ accumulation in shells, but 1 $mmol \cdot L^{-1}$ of KNO_3 could promote the cell growth.

Keywords: *Pleurochrysis carterae*, Calcium, Lipid, Carbohydrate, SEM (Scanning Electron Microscope), FTIR (Fourier-Transform Infrared Spectroscopy)

1. Introduction

Pleurochrysis carterae, also known as coccolithophorid, belongs to Haptophyta and is important to marine phytoplankton (Paasche 1968). *P. carterae* is a photoautotrophic unicellular marine alga. Cells are mostly round or oval and contain two chloroplasts (Johansen et al. 1988; Jordan and Chamberlain 1997). Like most photosynthetic organisms, *P. carterae* can synthesize organic material through photosynthesis, providing the necessary substances and energy for growth and reproduction.

During *P. carterae* growth, the cells form a scaly surface structure called coccolith, which is composed of $CaCO_3$ crystals formed via calcification. The reason why the coccolith exists is not clear. Some hypotheses include 1. To protect the cell; 2. To Reduce the effects of excessive light on algae growth; 3. To raise the refractive index when the light is insufficient; 4. To increase cell size; 5. To increase the sedimentation rate of cells; 6. To keep cells in a fixed water layer (Borowitzka 1977; Winter and Siesser 2006).

P. carterae was also found to contain high levels of lipids; the lipid content of *P. carterae* can reach 33% of dry weight (Moheimani and Borowitzka 2006). It contains many valuable ω - 3 Polyunsaturated Fatty Acids (PUFAs) (Chang et al. 2016), such as 18:3 ω-3, 18:4 ω-3, 18:5 ω-3, 20:4 ω-3, 20:5 ω-3 (Eicosapentaenoic Acid [EPA]), 22:5 ω-3, and 22:6 ω-3 (Docosahexaenoic Acid [DHA]). EPA and DHA have been shown to reduce cardiovascular disease (Simopoulos 2002) and they are highly valued for their health benefits.

Recent studies have also confirmed that *P. carterae* has great potential as a biodiesel producer (Ho et al. 2014; Moheimani and Borowitzka 2006; Ratledge and Cohen 2008).

Under suitable growth conditions, *P. carterae* could bloom, releasing many volatile substances such as Dimethyl Sulfide (DMS) and acrylic acid. Algal blooms affect the local environment, ecosystem, and marine economy (Zhou et al. 2008a). Water-enriching nutrients (N, P^{3-}, K^{+}) result in eutrophication of the sea, one of the leading causes of algal blooms (Anderson et al. 2002). Potassium is a variety of enzyme activator, plays an important role in metabolism: promote photosynthesis, promote nitrogen metabolism, improve plant nitrogen absorption. KNO_3 has not only potassium but also nitrogen; it is a very important nutrient for microalgae.

This study focuses on the effects of KNO_3 on $CaCO_3$ accumulation, lipid accumulation, carbohydrate and protein content of *P. carterae.* Some researchers found that when the concentration of KNO_3 is 0.9 mM, *Nannochloris sp.* can accumulate more lipids than a medium containing 2.0–9.9 mM KNO_3 (Takagi et al. 2000). Based on the previous study on *Nannochloris sp.* we propose that low concentration of KNO_3 could promote lipid accumulation in *P. carterae*, and also could promote the $CaCO_3$ content.

2. Materials and methods

2.1. Algal strain

Pleurochrysis carterae was purchased from National Center for Marine Algae and Microbiota (NCMA - https://ncma.bigelow.org/ccmp646) (Kindly provided by Dr. Fan Lu, Hubei University of Technology, China).

2.2. Preparation of f/2 medium

The f/2 medium (pH 8.0) contains 225 $mg \cdot L^{-1}$ $NaNO_3$, 5.6 $mg \cdot L^{-1}$ $NaH_2PO_4 \cdot H_2O$, 1 $ml \cdot L^{-1}$ trace metal solution, and 0.5 $ml \cdot L^{-1}$ vitamin solution. The trace metal solution is

composed of 315 mg $FeCl_3 \cdot 6H_2O$, 436 mg $Na_2EDTA \cdot 2H_2O$, 9.8 mg $CuSO_4 \cdot 5H_2O$, 6.3 mg $Na_2NoO_4 \cdot 2H_2O$, 22 mg ZnSO4·7H_2O, 10 mg $CoCl_2 \cdot 6H_2O$, and 180 mg $MnCl_2 \cdot 4H_2O$ dissolved in a final volume of 100 ml distilled water. The vitamin solution is composed of 20 mg thiamine HCl (vitamin B_1), 10 mg biotin (vitamin H), and 10 mg cyanocobalamin (vitamin B_{12}) dissolved in a final volume of 100 ml distilled water.

2.3. Algal culturing

P. carterae were cultured in f/2 medium (Guillard and Ryther 1962) with different concentrations of KNO_3 (0.25, 0.5, 0.75, 1 $mmol \cdot L^{-1}$), without KNO_3 used as a control and each concentration has three replicates. The starting algal cell density was 1.5×10^5 cells per liter. The culture temperature was set at 26°C with 16/8 hours light and dark photocycle provided by cold white fluorescent light and 24 hours continuous air pumping.

2.4. Sample collection

Two hundred milliliters (200 ml) of *P. carterae* cells were collected by centrifugation at 5,000 $r \cdot min^{-1}$ for 10 minutes at days 0, 2, 4, 6, 8, 10. The pellets were washed twice with distilled water, and the samples were dried in oven at 105 ℃ until the weight remained stable.

2.5. *P. carterae* calcium content measurement

2.5.1. Sample decolorization

The samples were decolorized with 75% ethanol before measuring the calcium content (Corstjens and Gonzalez 2004; Daugbjerg and Andersen 1997; Dyhrman et al. 2006). One ml of ethanol was added into 0.01 mg of the dry algae. After 30 minutes of the water bath (80 ℃), the samples were collected by centrifugation at 12,000 $r \cdot min^{-1}$ for 30

minutes. The supernatant was then discarded, and the steps were repeated until the supernatant was colorless.

2.5.2. Calcium content measurement of decolorization samples

Decolorized samples were mixed with 1.5 ml of 2 N HCl followed by a water bath (80 ℃) for 30 minutes to remove CO_2. The supernatant containing $CaCl_2$ was collected by centrifugation at 12,000 r·min^{-1} for 3 minutes. The calcium ion content in the supernatant was measured by the Ethylenediaminetetraacetic Acid (EDTA) complexometric titration method (Wang et al. 2007). The end-point was recorded and determined by observing when the color of the Calconcarboxylic Acid (Calcon indicator) changed from red to blue and remained for at least 30 seconds. Calcium ion content (mg·L^{-1}) was calculated according to the following equation 1:

$$\mathrm{Ca} = \frac{\mathrm{M}\times\mathrm{a}\times 40.08}{\mathrm{V}} \times 1000 \qquad \text{Equation 1}$$

M: EDTA standard solution molar concentration

a: The volume (ml) of EDTA standard solution is consumed during the titration

V: Sample volume (ml)

The atomic weight of calcium: 40.08

The calcium ion content in the sample is calculated based on the standard curve.

2.6. Total lipid measurement

Lipids were extracted by using the chloroform-methanol extraction method (Bligh and Dyer 1959). Dry algae powder of 0.01 g was transferred to a 1.5 ml centrifuge tube. Then, 395 µl chloroform, 790 µl methanol, and 316 µl deionized water were added, to make a ratio of 1:2:0.8 (V: V: V). This was then mixed by vortex for 3 to 5 minutes, followed by

3 minutes of centrifugation at 12,000 r·min^{-1}. The supernatant was collected in a glass tube, and the above operation was repeated three more times.

Once all supernatant was collected in a 15 ml glass tube, chloroform, methanol, and water were added to make the final volume ratio 1: 1: 0.9 (V: V: V). The solution was mixed well and left until complete phase separation occurred. The bottom layer was then collected to a pre-weighed tube, recorded as M1 (g), and placed in the fume hood overnight. The tube was further dried in oven at 105 ℃ until the weight was constant, then weighed and recorded as M2 (g). The lipid content was calculated according to following equation 2:

$$\text{Lipids content (\%)} = \frac{\text{M2 (g)} - \text{M1(g)}}{\text{0.01 (g)}} \times 100\% \qquad \text{Equation 2}$$

2.7. Carbohydrate content measurement

The phenol-sulfuric acid method was used for carbohydrate content measurement (Cuesta et al. 2003). The dry algal powder samples of 0.01g were mixed with 2 ml distilled water and 600 µl concentrated HCl in a 15 ml centrifugation tube, followed by a water bath (100 °C) for 3 hours. It was then cooled to room temperature and filtered, and the residue was washed with distilled water three times. The residue was re-suspended using 10 ml of distilled water and centrifugation at 12,000 r·min^{-1} for 2 minutes. All supernatant was collected for total sugar determination. The 5 % phenol solution of 1 ml was added to 2 ml supernatant and shaken well. Then 5 ml of concentrated sulfuric acid was quickly added and let stand for 10 minutes. Vortex was used to mix evenly before placing in a water bath at 40 °C for 30 minutes, followed by a cold-water bath for 5 minutes. The absorbance was measured at 490 nm using distilled water as a blank in an Epoch™

Microplate Spectrophotometer (BioTek®, Inc., headquartered in Winooski, VT, USA).

2.8. Extraction and determination of protein content

For protein content determination, SK3041-1000 Assays Better Bradford Protein assay kit was used according to the manufacturer's instructions (Bio Basic Canada Inc., Markham, ON, CA). Algal powder of 0.01 g was added to a 2 ml centrifugation tube, and then 1 ml of 0.15 M NaCl solution was added to re-suspend the algal powder, followed by the sonification at 40 kHz on ice for 10 minutes. After that, the tubes were centrifuged at 12,000 $r \cdot min^{-1}$ for 2 minutes. The pellets were washed three times using distilled water, then using 0.15 M NaCl solution to extract the protein. The protein extraction was collected by centrifugation at 12,000 $r \cdot min^{-1}$ for 5 minutes. The supernatant containing the proteins was kept on ice for protein measurement. The supernatant (150 µl) was mixed with 150 µl Bradford reagent and kept at room temperature for 15 minutes. The absorbance at 595 nm was determined using an Epoch™ Microplate Spectrophotometer (BioTek®, Inc., headquartered in Winooski, VT, USA). A range of BSA (0-30 $mg \cdot ml^{-1}$) concentration was used to plot the standard curves for the protein assay.

2.9. Scanning Electron Microscope (SEM) sample preparation

2.9.1. Sample fixation and dehydration procedure

The algal samples were placed in the solution of 2.5 % to 3 % concentration of glutaraldehyde in phosphate buffer (usually at a pH of around 6.8 to 7.4) (Calvert et al. 1976) for 30 minutes to ensure complete infiltration of the glutaraldehyde solution into the *P. carterae*. The fixed *P. carterae* were subjected to gradient dehydration with 50 %, 60 %, 70 %, 80 %, 90 %, and 100 % concentrations of ethanol. The sample was soaked in

each concentration for at least 15 minutes, increasing from lowest to highest concentration. The sample was then kept in a -80 ℃ freezer until use.

2.9.2. Scanning Electron Microscope (SEM)

The samples were removed from the -80°C freezer, then placed into a freezing dryer (LABCONCO freezone 12, Kansas City, MO, USA) for 24 hours. The samples were then sputtered with gold or carbon, using HITACHI SU-70 Scanning Electron Microscope for imaging.

2.10. Fourier-Transform Infrared Spectroscopy (FTIR)

For further verify the accuracy of experimental results, FTIR (BRUKER TENSOR 37) was used to verify carbohydrate, protein, and lipid content, and each sample preform triplications. The characteristic absorption band of lipids is around 3000-2800 cm^{-1} (representing the C-H stretching vibration in acyl chains) which can well-characterize the lipid content changes. The protein C=O stretching vibrations and N-H bending vibrations are represented by bands at 1650 cm^{-1} (amide I) and 1540 cm^{-1} (amide II), respectively. The changes in absorption correspond to protein content. The carbohydrate absorption bands at 1200-950 cm^{-1} represent the C-O-C vibration, and this absorption strength can be used to observe the changes of total carbohydrate content (Giordano et al. 2001; Meng et al. 2014; Pistorius et al. 2009).

3. Results

3.1. The effect of KNO_3 on $CaCO_3$ accumulation of *P. carterae*

The *P. carterae* were measured for calcium content, lipid content, carbohydrate content, and protein content on days 0, 2, 4, 6, 8, 10. The calcium content of *P. carterae* is

generally around 10 % (Jorquera et al. 2010; Moheimani and Borowitzka 2006). *P. carterae* exhibited two phases, calcifying phase and non-calcifying phase (Marsh 2003; Zhou et al. 2008b). *P. carterae* do not accumulate coccolith on the cell surface in the early stages of growth or when undernourished and there was no calcium carbonate shell on the cell surface. *P. carterae* was surrounded by calcium carbonate shells once it was well-nourished or in the late growth stage (Zhou et al. 2008b). The standard curve for calcium ion content is shown in Fig. 1.

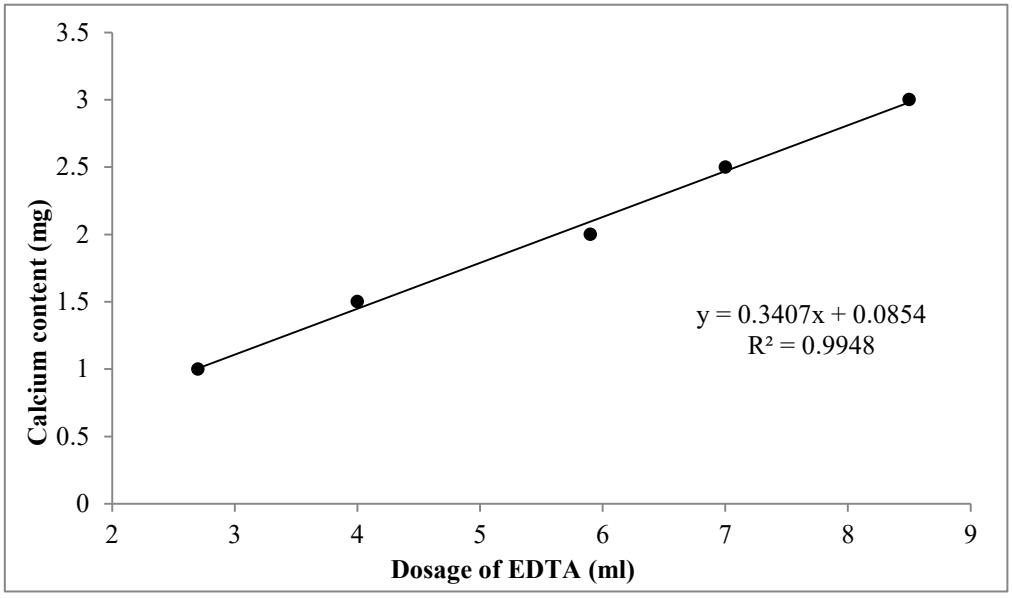

Fig. 1 Calcium ion content standard curve

On day 10, the calcium content reached the maximum under the different KNO_3 culture conditions, respectively (Fig. 2A). On day 10, when KNO_3 concentration was 0.75 $mmol \cdot L^{-1}$, *P. carterae* accumulated more calcium carbonate, around 10.01 % of dry weight (Fig. 2B).

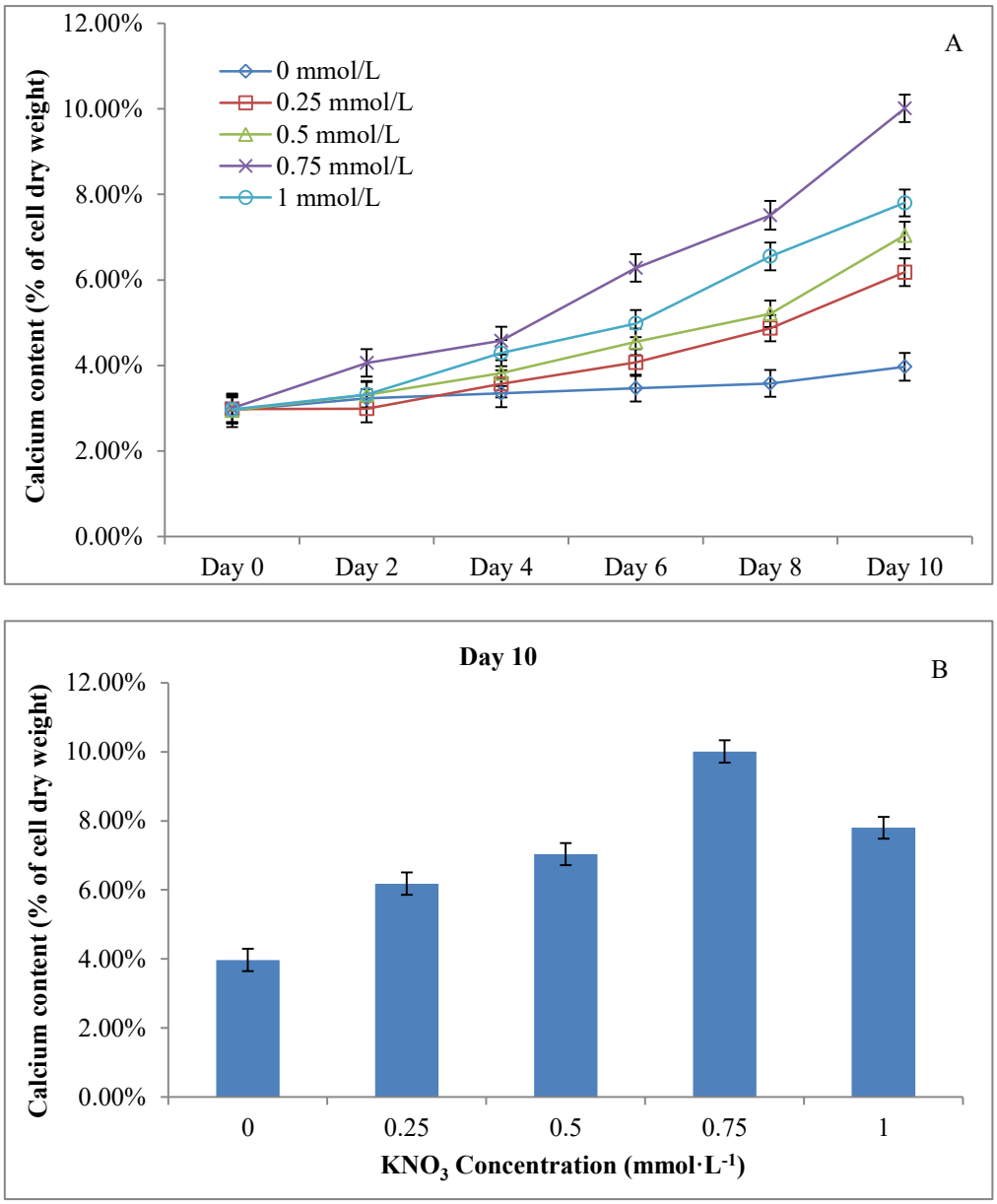

Fig. 2A/B A: Ten days' calcium content trend of *P. carterae* growing in f/2 medium containing different concentrations of KNO_3 (0, 0.25, 0.5, 0.75, and 1 $mmol \cdot L^{-1}$); **B:** Calcium content of *P. carterae* in different KNO_3 concentration culture mediums on day 10.

To confirm day 10 calcification trend results, SEM was used to observe the extracellular calcification (Fig. 3). At the same magnification, the changes in $CaCO_3$ content on the surface of *P. carterae* were clearly observed (Fig. 3 a - e). From SEM results, in the

control group, *P. carterae* were not covered with calcium carbonate (Fig. 3a). From Fig. 3d, When KNO_3 was at 0.75 mmol·L^{-1}, the algal cells had the largest size and most coccolith coverages was observed. Compared to other concentration of KNO_3 When *P. carterae* cultured under 1 mmol·L^{-1} of KNO_3, the cells were more individual (Fig. 3 a-1 to e-1). However, cell size and $CaCO_3$ content were less than the 0.75 mmol·L^{-1} of KNO_3 cultured *P. carterae*. In Fig. 3 a-1 to e-1, Fig. 3 d-1 showed the largest cell number. Although the cell number of c-1 was more than e-1, the surface of the e-1 cell had more coccolith. Only a small amounts of calcium carbonate accumulated on the cell surface on day 10 (Fig. 3 a-1), when the medium which did not contain extra potassium nitrate on day 10.

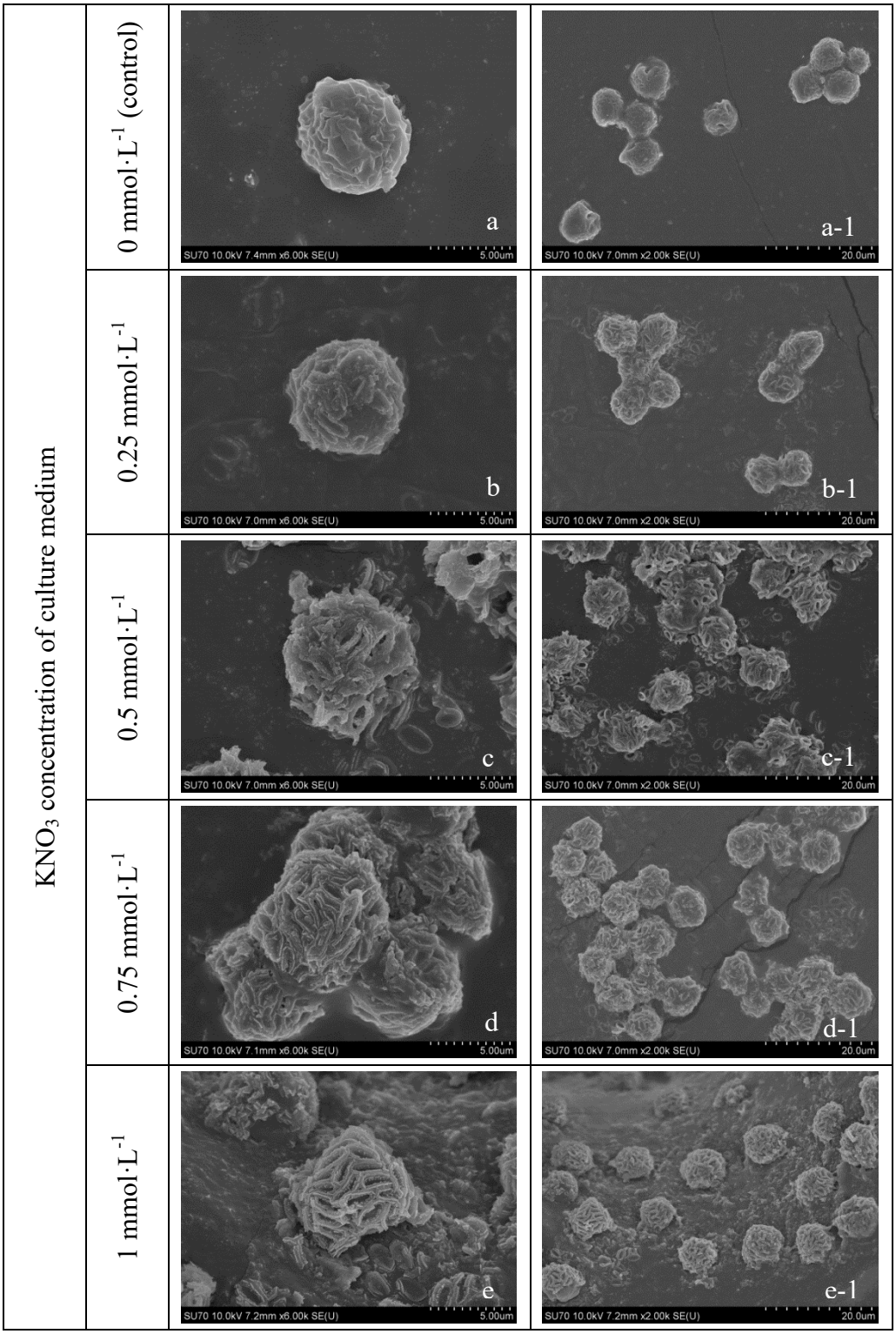

Fig. 3 SEM picture of different KNO_3 concentrations of f/2 medium cultured *P. carterae* on day 10

3.2. The effect of KNO_3 on lipid accumulation of *P. carterae*

Lipid accumulation of *P. carterae* gradually increased from day 0 to day 10 (Fig. 4 A/B).

P. carterae accumulated the highest lipid content was shown in the medium without additional KNO_3 on day 10 (Fig. 4B). Under 1 mmol·L^{-1} concentration of KNO_3, *P. carterae* has only a small amount of lipid accumulation and lipid content of 13.67 % on day 10. In the f/2 medium, the lipid content of *P. carterae* accounted for 33 % of dry weight (Endo et al. 2016; Moheimani and Borowitzka 2006). My study found the lipid content of *P. carterae* was 33.61 % of dry weight on day 10 in the medium without KNO_3, similar to previous research.

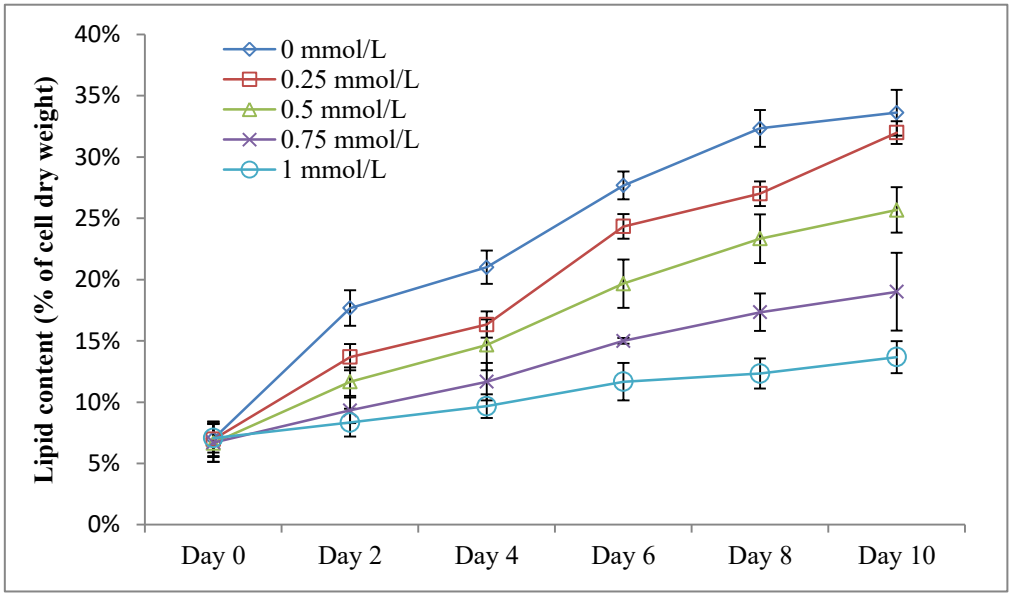

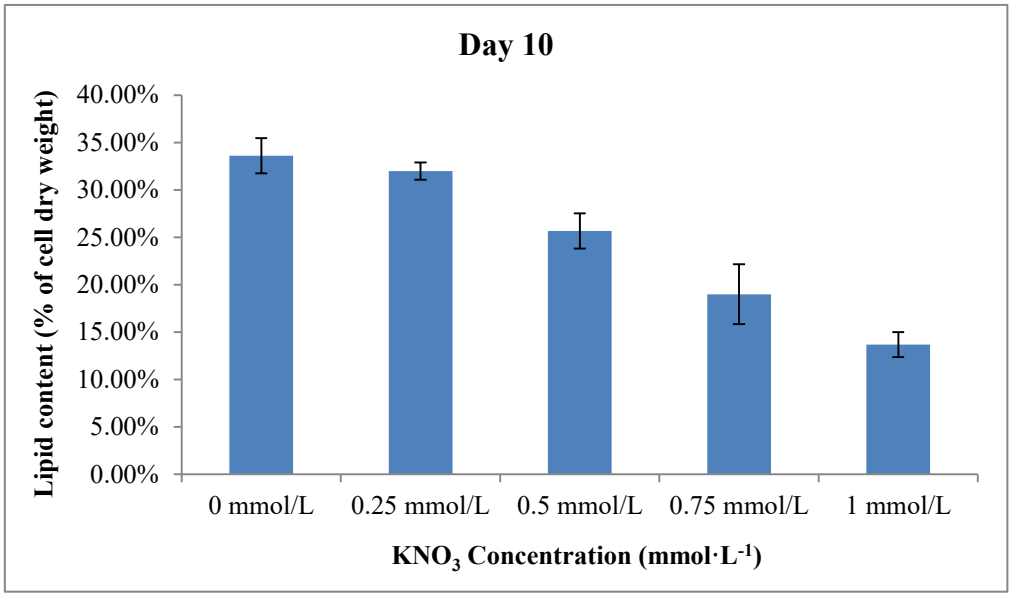

Fig. 4A/B A: Ten days' lipid content trend of *P. carterae* growing in f/2 medium containing different concentrations of KNO_3 (0, 0.25, 0.5, 0.75, and 1 $mmol \cdot L^{-1}$); **B:** Lipid content of *P. carterae* in different KNO_3 concentration culture mediums on day 10.

3.3. The effect of KNO_3 on total carbohydrate content of *P. carterae*

Carbohydrate content in microalgae generally accounts for 5 % to 23 % of dry weight (Jie-qiong et al. 2016). There was no deliberate addition of potassium ions in the f/2 medium used (Guillard and Ryther 1962).

After 10 days of cultivation, the carbohydrate content of *P. carterae* decreased with higher concentrations of KNO_3 (Fig. 5A). The lowest carbohydrate content occurred when 1 $mmol \cdot L^{-1}$ of KNO_3 was added to the f/2 medium. From 0 to 0.25 $mmol \cdot L^{-1}$ concentration of KNO_3, the carbonate content of dry weight was higher than 30 % (Fig. 5B). The carbohydrate content of the control group (0 $mmol \cdot L^{-1}$) on day 10 accounted for 33.70 % of the dry weight. In contrast, the carbohydrate content of *P. carterae* accounted for 21.08 % of the dry weight, and under 1 $mmol \cdot L^{-1}$ potassium nitrate on day 10, the carbohydrate content of 12.62 % less compared to the control group (Fig. 5B).

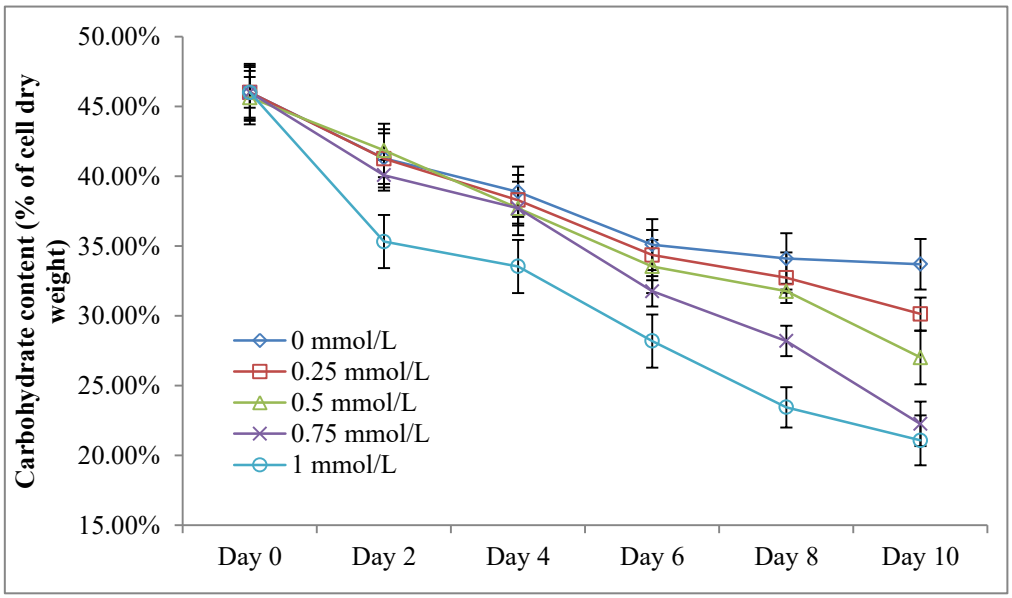

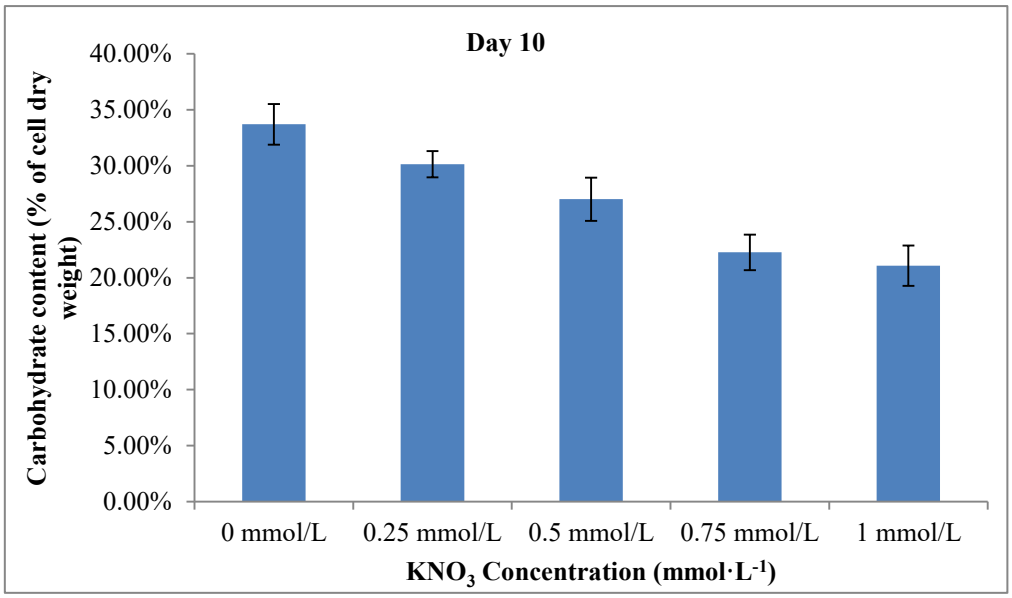

Fig. 5A/B A: Ten days' carbohydrate content trend of *P. carterae* growing in f/2 medium containing different concentrations of KNO_3 (0, 0.25, 0.5, 0.75, and 1 mmol·L^{-1});

B: Carbohydrate content of *P. carterae* in different KNO_3 concentration culture mediums on day 10.

3.4. The effect of KNO_3 on the total protein content of *P. carterae*

The 10-day protein content trend of *P. carterae* is shown in Fig. 6A. On day 10, the optimum concentration for total protein content was 1 mmol·L^{-1}; protein content reached 32.87 % of dry weight (Fig. 6B). When the KNO_3 was 0 to 0.5 mmol·L^{-1}, the protein content in *P. carterae* was lower than 30 % of dry weight. The protein content of the control group on day 10 accounted for 27.21 % of the dry weight, 5.66 % lower than the highest content (Fig. 6B).

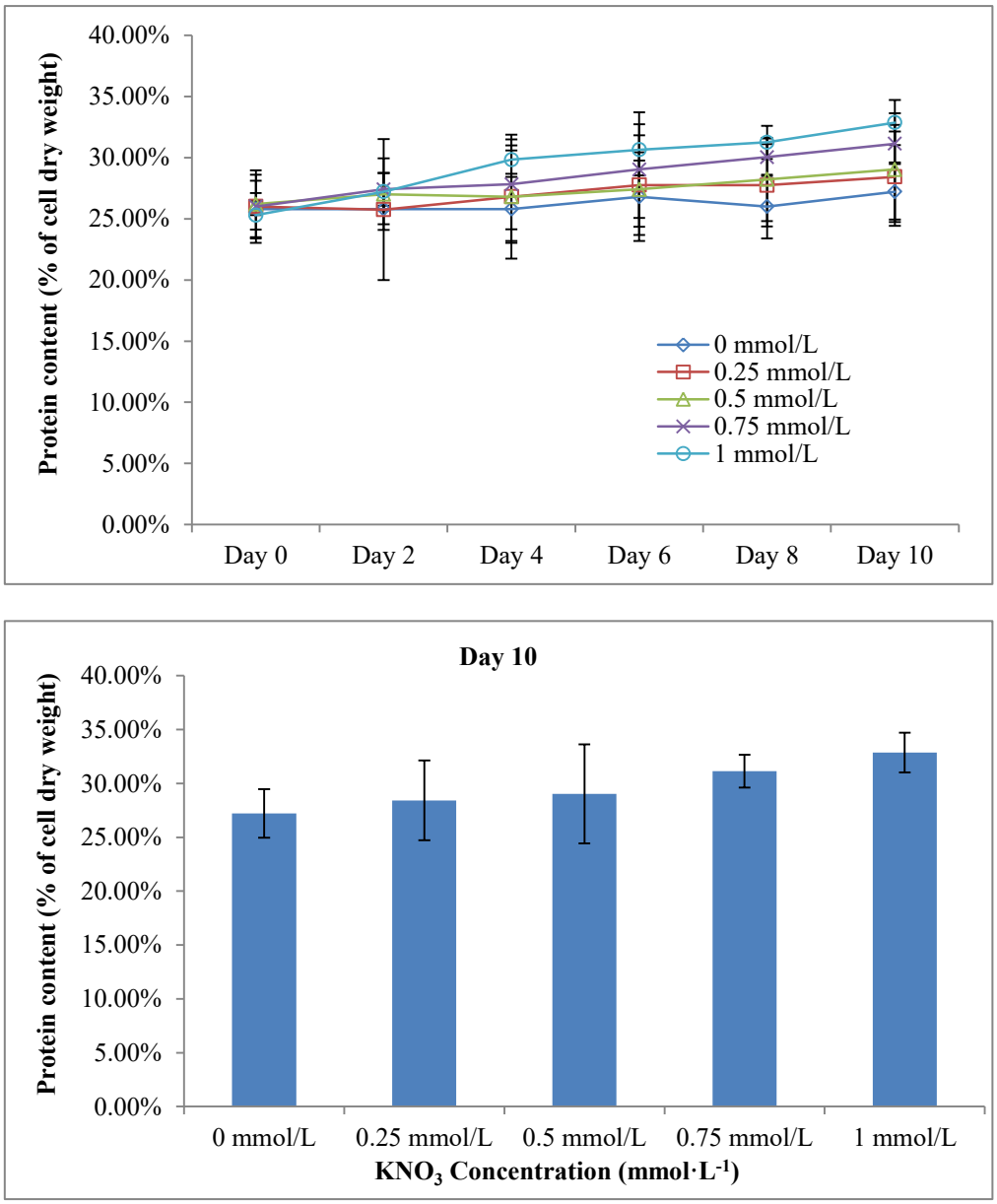

Fig. 6A/B A: Ten days' protein content trend of *P. carterae* growing in f/2 medium containing different concentrations of KNO_3 (0, 0.25, 0.5, 0.75, and 1 $mmol \cdot L^{-1}$); **B:** Protein content of *P. carterae* in different KNO_3 concentration culture mediums on day 10.

3.5. Fourier-transform infrared spectroscopy (FTIR) results

To verify the results of lipid content, protein content, and carbohydrate content, the FTIR test was performed on day 10 (Fig. 7). The peaks indicated by the three arrows represent

carbohydrates (1072 cm^{-1}), proteins (1649 cm^{-1}), and lipids (2953 cm^{-1}), respectively. The FTIR results can measure changes of the carbohydrates, proteins, lipids, and the transmittance is negatively related to these product content (Giordano et al. 2001; Meng et al. 2014; Pistorius et al. 2009).

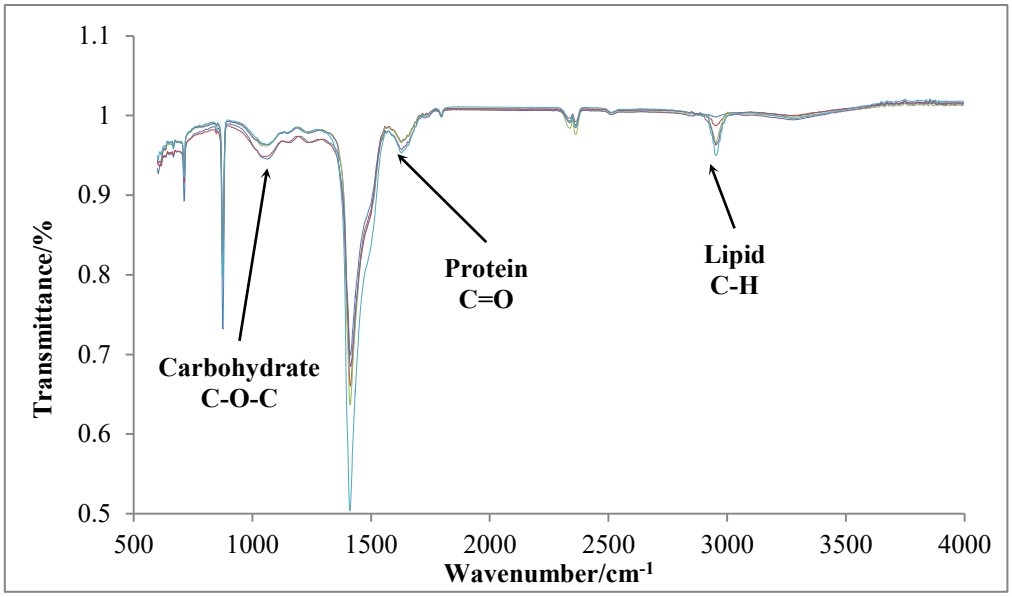

Fig. 7 FTIR results on day 10

The light transmittance results for the three products are shown in Table 1. Table 1 shows that the light transmittances of lipid have 99.81 % in the medium contains 1 $mmol \cdot L^{-1}$ of KNO_3 (It has a similar trend with Fig. 4B). When the medium without potassium nitrate, 97.24 % of light transmittances of proteins in *P. carterae* were measured with FTIR (It has a similar trend with Fig. 6B).The light transmittance of carbohydrate was 96.42 % at 1 $mmol \cdot L^{-1}$ of KNO_3 (It has a similar trend with Fig. 5B). Based on the result of analysis of variance (ANOVA) all the samples in carbohydrate and lipid sections have significant differences between 0 $mmol \cdot L^{-1}$and other concentrations respectively. However, in protein sections, we do not have significant differences between 0 and 0.25, 0.5 $mmol \cdot L^{-1}$ ($P < 0.05$).

Absorption \ KNO_3	0 mmol·L^{-1}	0.25 mmol·L^{-1}	0.5 mmol·L^{-1}	0.75 mmol·L^{-1}	1 mmol·L^{-1}
Lipid (2953 cm^{-1})	95.01±0.02%	96.31±0.02%	96.44±0.02%	98.75±0.02%	99.81±0.03%
Protein (1649 cm^{-1})	97.24±0.03%	97.21±0.01%	97.20±0.02%	96.34±0.01%	95.98±0.01%
Carbohydrate (1072 cm^{-1})	94.64±0.02%	94.99±0.01%	96.28±0.02%	96.40±0.02%	96.42±0.01%

Table 1 Transmittance rate of three products under different concentrations of KNO_3

4. Discussion

In this research, the effects of various concentrations of potassium nitrate (0.25, 0.5, 0.75, and 1 mmol·L^{-1}, without potassium nitrate as control) on $CaCO_3$ accumulation, lipid accumulation, carbohydrate content, and protein content in *P. carterae* were studied.

When KNO_3 was 0.75 mmol·L^{-1}, *P. carterae* accumulated the highest $CaCO_3$ content, around 10.01 % of dry weight on day 10 (Fig. 2 A/B). However, the control group (0 mmol·L^{-1}) had the lowest calcium content, about 3.97 % (Fig. 2B). To verify the titration methods results, we observed the cell surface calcification of the day 10 samples by using SEM (Fig. 3). The calcification trends of *P. carterae* shown in the SEM were almost identical to the calcium content trends of *P. carterae* (Fig. 2B).

According to the SEM results, KNO_3 had an important effect on $CaCO_3$ synthesis in *P. carterae*; within the range of 0 to 0.75 mmol·L^{-1}, the more KNO_3 present, the more calcium carbonate accumulated by *P. carterae*. SEM results are similar to the results of titration methods. This suggests that the 0.75 mmol·L^{-1} of KNO_3 helped *P. carterae* synthesize the calcium carbonate shell earlier. Under 1 mmol·L^{-1} of KNO_3, algal cells were completely independence (Fig. 3 e-1); However, *P. carterae* cultured in potassium

nitrate with a concentration of less than 1 mmol·L^{-1} exhibited agglomeration.

We propose that with 1 mmol·L^{-1} KNO_3 in the medium, the cells can enter the active period earlier, but the calcium content of the cells and the size of the cells could be reduced relative to lower NKO_3 concentrations. This suggests that too much K^+ disrupts the uptake of calcium (Lovejoy 2018).

Previous studies have found that the percentage of total algal protein in dry weight ranges from 3.19 % to 78.10 % (Burtin 2003; Fernández-Reiriz et al. 1989; Piorreck et al. 1984; Sánchez-Machado et al. 2004). Other researchers also found that the protein content of *P. carterae* accounts for 28.8 % of dry weight when cultured in Eppley medium (Nishimori and Morinaga 1996). During 10 days of cultivation, the total protein content of *P. carterae* increased with increasing concentrations of potassium nitrate (Fig. 6A). Whereas, the lipid and sugar content of *P. carterae* decreased with increasing concentrations of KNO_3 (Fig. 4A, 5A). If the concentration of KNO_3 was increased, the accumulation of lipids in *P. carterae* was reduced. I am suggesting that the lipid accumulation in *P. carterae* was inversely correlated within the range of 0 to 1 mmol·L^{-1} concentration of KNO_3. To further verify the results, the FTIR was used to detect the content of the three products. A comparison of the FTIR results (Table 1) with the results from the previous methods (Fig. 6B) revealed a positive correlation between the protein content and the potassium nitrate content. Which means KNO_3 was negatively correlated with lipid and sugar content. When the potassium nitrate concentration is 1 mmol·L^{-1}, *P. carterae* is more fragmented (Fig. 3 e-1).

When the potassium nitrate concentration in the medium was 0.75 mmol·L^{-1}, *P. carterae*

accumulate the highest calcium carbonate content, but for the highest protein accumulation, the optimum potassium nitrate concentration should be 1 $mmol \cdot L^{-1}$. However, for more lipid and sugar accumulation, better do not add extra KNO_3 to the medium. Moreover, *P. carterae* cells had higher growth activity when potassium nitrate concentration was 1 $mmol \cdot L^{-1}$.

From the above results, when *P. carterae* blooms due to excessive KNO_3, its cells should contain more calcium, which can be collected to obtain $CaCO_3$. If want to get more lipids, it is not recommended to collect *P. carterae* when a bloom occurs.

5. References

Anderson DM, Glibert PM, Burkholder JM. (2002). Harmful algal blooms and eutrophication: nutrient sources, composition, and consequences. Estuaries, 25:704-726

Bligh EG, Dyer WJ. (1959). A rapid method of total lipid extraction and purification. Canadian Journal of Biochemistry and Physiology, 37:911-917

Borowitzka MM. (1977). Algal calcification. Oceanography and Marine Biology: an Annual Review-Pages, 15: 189-223

Burtin P. (2003). Nutritional value of seaweeds Electronic journal of Environmental. Agricultural and Food Chemistry, 2:498-503

Calvert HE, Dawes CJ, Borowitzka MA. (1976). Phylogenetic relationships of Caulerpa (Chlorophyta) based on comparative chloroplast ultrastructure. Journal of Phycology, 12:149-162

Chang KJL, Dunstan GA, Mansour MP, Jameson ID, Nichols PD. (2016). A novel series of C 18–C 22 trans ω3 PUFA from Northern and Southern Hemisphere strains of the marine haptophyte Imantonia rotunda. Journal of Applied Phycology, 28:3363-3370

Corstjens PL, Gonzalez EL. (2004). Effects of nitrogen and phosphorus availability on the expression of the coccolith-vesicle V-ATPase (subunit c) of Pleurochrysis (Haptophyta). Journal of Phycology, 40:82-87

Cuesta G, Suarez N, Bessio MI, Ferreira F, Massaldi H. (2003). Quantitative determination of pneumococcal capsular polysaccharide serotype 14 using a

modification of phenol–sulfuric acid method. Journal of Microbiological Methods, 52:69-73

Daugbjerg N, Andersen RA. (1997). Phylogenetic analyses of the rbcL sequences from haptophytes and heterokont algae suggest their chloroplasts are unrelated. Molecular Biology and Evolution, 14:1242-1251

Dyhrman ST, Haley ST, Birkeland SR, Wurch LL, Cipriano MJ, McArthur AG. (2006). Long serial analysis of gene expression for gene discovery and transcriptome profiling in the widespread marine coccolithophore Emiliania huxleyi. Applied and Environmental Microbiology, 72:252-260

Endo H, Yoshida M, Uji T, Saga N, Inoue K, Nagasawa H. (2016). Stable nuclear transformation system for the Coccolithophorid alga Pleurochrysis carterae. Scientific Reports, 6:22252

Feng P, Deng Z, Fan L, Hu Z. (2012). Lipid accumulation and growth characteristics of Chlorella zofingiensis under different nitrate and phosphate concentrations. Journal of Bioscience and Bioengineering, 114:405-10.

Fernández-Reiriz MJ, Perez-Camacho A, Ferreiro M, Blanco J, Planas M, Campos M, Labarta U. (1989). Biomass production and variation in the biochemical profile (total protein, carbohydrates, RNA, lipids and fatty acids) of seven species of marine microalgae. Aquaculture, 83:17-37

Giordano M, Kansiz M, Heraud P, Beardall J, Wood B, McNaughton D. (2001). Fourier transform infrared spectroscopy as a novel tool to investigate changes in intracellular macromolecular pools in the marine microalga Chaetoceros muellerii

(Bacillariophyceae). Journal of Phycology, 37:271-279

Guillard RR, Ryther JH. (1962). Studies of marine planktonic diatoms: I. Cyclotella nana Hustedt, and Detonula confervacea (Cleve) Gran. Canadian journal of microbiology, 8:229-239

Ho DP, Ngo HH, Guo W. (2014). A mini review on renewable sources for biofuel. Bioresource technology, 169:742-749

Jie-qiong L, Hong-quan L, Sha Y. (2016). Research progress of microalgae polysaccharide. Modern Chemical Industry, 60-62

Johansen JR, Doucette GJ, Barclay WR, Bull JD. (1988). The morphology and ecology of Pleurochrysis carterae var. dentata var. nov.(Prymnesiophyceae), a new coccolithophorid from an inland saline pond in New Mexico, USA. Phycologia, 27:78-88.

Jordan R, Chamberlain A. (1997). Biodiversity among haptophyte algae. Biodiversity & Conservation, 6:131-152

Jorquera O, Kiperstok A, Sales EA, Embirucu M, Ghirardi ML. (2010). Comparative energy life-cycle analyses of microalgal biomass production in open ponds and photobioreactors. Bioresource Technology, 101:1406-1413

Lovejoy R. (2018). Ways to treat high potassium in soil. home guide SF gate. http://homeguides.sfgate.com/ways-treat-high-potassium-soil-102992.html. Accessed 20 May 2018

Marsh M. (2003). Regulation of CaCO3 formation in coccolithophores. Comparative Biochemistry and Physiology Part B: Biochemistry and Molecular Biology,

136:743-754

Meng Y, Yao C, Xue S, Yang H. (2014). Application of Fourier transform infrared (FT-IR) spectroscopy in determination of microalgal compositions. Bioresource Technology, 151:347-54.

Moheimani NR, Borowitzka MA. (2006). The long-term culture of the coccolithophore Pleurochrysis carterae (Haptophyta) in outdoor raceway ponds. Journal of Applied Phycology, 18:703-712

Nishimori T, Morinaga T. (1996). Safety evaluation of Pleurochrysis carterae as a potential food supplement. J Mar Biotechnol, 3:274-277

Paasche E. (1968). Biology and physiology of coccolithophorids. Annual Reviews in Microbiology, 22:71-86.

Piorreck M, Baasch KH, Pohl P. (1984). Biomass production, total protein, chlorophylls, lipids and fatty acids of freshwater green and blue-green algae under different nitrogen regimes. Phytochemistry, 23:207-216

Pistorius A, DeGrip WJ, Egorova-Zachernyuk TA. (2009). Monitoring of biomass composition from microbiological sources by means of FT-IR spectroscopy. Biotechnology and Bioengineering, 103:123-129

Ratledge C, Cohen Z. (2008). Microbial and algal oils: do they have a future for biodiesel or as commodity oils? Lipid Technology, 20:155-160

Sánchez-Machado D, López-Cervantes J, Lopez-Hernandez J, Paseiro-Losada P. (2004). Fatty acids, total lipid, protein and ash contents of processed edible seaweeds. Food Chemistry, 85:439-444

Simopoulos AP. (2002). Omega-3 fatty acids in inflammation and autoimmune diseases. Journal of the American College of Nutrition, 21:495-505

Takagi M, Watanabe K, Yamaberi K, Yoshida T. (2000). Limited feeding of potassium nitrate for intracellular lipid and triglyceride accumulation of Nannochloris sp. UTEX LB1999. Applied Microbiology and Biotechnology, 54:112-117

Wang ZF, Song BC, Zhang J. (2007). Precise Measurement of Ca and P Content in Hydroxyapatite by Chemical Analysis [J]. Bulletin of the Chinese Cerrmic Society, 1:040

Winter A, Siesser WG. (2006). Coccolithophores. Cambridge University Press.

Zhang WJ, Shi DJ, Guo LC. (2004). Effects of Theree Nutrition Salts on Growth of Pleurochrysis Carterae. Sea Lake Salt and Chemical Industry, 33:16-19

Zhou CX, Yan XJ, Sun X, Xu JL, Fu YJ. (2008a). The experimental observations and characteristics of one strain of coccolithophorid from the bloom water in a shrimp pool, ZheJiang, CHINA. Acta Hydrobiologica Sinica, 6:025.

Zhou C, Yan X, Luo Q, Ma B. (2008b). population growth characteristics and relevant biochemical changes of coccolithophorid (Pleurochrysis sp.)at low and high temperatures. Acta Ecologica Sinica, 2587-94.

CHAPTER IV

A Novel Coccolith Structure Formed in *Pleurochrysis carterae* by $CaCO_3$ Accumulation

Xuantong Chen[1, 2], Chonlong Chio[1], Fan Lu[3], Wensheng Qin[1*]

[1]Department of Biology, Lakehead University, 955 Oliver Road, Thunder Bay, Ontario, P7B 5E1, Canada.

[2]Faculty of Natural Resources Management, Lakehead University, 955 Oliver Road, Thunder Bay, Ontario, P7B 5E1, Canada.

[3]School of Civil Engineering, Architecture and Environment, Hubei University of Technology, Wuhan, 430068, China.

* Corresponding author: wqin@lakeheadu.ca

Abstract

Pleurochrysis carterae is a marine alga, widely distributes in oceans. The *P. carterae* cell is covered by many individual coccoliths which are mainly composed of calcium carbonate ($CaCO_3$). One of the major threats to marine ecosystems is ocean acidification which is the result of carbon dioxide (CO_2) from the atmosphere is absorbed by the oceans. During coccolith accumulation and photosynthesis process, *P. carterae* absorbs CO_2 from the environment. Thus *P. carterae* could play an important role in the carbon cycle. This study revealed that the accumulation of $CaCO_3$ on the shells of *P. carterae* developed a special planar structure, named "doornail structure", in the inner tube of the R unit, parallel with the outer tube of the V unit. The double-disc of adjacent coccolith cross each other, and such a cross-structure ensures that each coccolith cannot move freely in a horizontal direction, so each coccolith is

fixed and form a support structure. Furthermore, this cross-structure can be stretched and not damaged by the expansion of the protoplasts during the division of the cell. This is the first research that revealing how coccolith protects and supports the *P. carterae* cells.

Keywords: *Pleurochrysis carterae,* SEM (Scanning Electron Microscope), doornail structure, cross structure, V unit, R unit

1. Introduction

The ocean plays a significant role in the global carbon cycle by absorbing carbon dioxide (CO_2) emission from anthropogenic activities. However, the dissolution of CO_2 is leading to a decrease of the pH in aquatic environments, particularly in the oceans. One-third of the CO_2 released by human activities is absorbed by the oceans from the atmosphere (Sabine et al. 2004) and forms carbonic acid leading to ocean acidification, one of the major threats to marine ecosystems (Fabry et al. 2008). Moreover, the increasing levels of carbon dioxide in the atmosphere can cause changes in the pH of the ocean surface, which slows the calcification process of algae. (Riebesell et al. 2000). Particularly, coccolithophorid including the species *Pleurochrysis carterae* is calcifying organisms which can produce calcium carbonate ($CaCO_3$) using CO_2 in the aquatic environment (Riebesell et al. 2000). Thus, coccolithophorid is abundant phytoplankton which is responsible for the production of a large part of modern oceanic carbonate (Riebesell et al. 2000).

Pleurochrysis carterae is a marine coccolithophorid (*Prymnesiophyceae*); it is a major group of calcifying algae, belonging to the phylum Haptophyta (Beech and Wetherbee 1984). *P. carterae* is a unicellular flagellated golden or yellow-green alga capable of producing coccolith, a special structure of calcite plates within vesicle where an interlocking is produced on its cell wall's exterior surface. In many organisms, the functional materials of biofabrication are an inherent process, and lots of the forms and composition of biominerals has been learned (Marsh 1999a; Marsh 1999b; Lowenstam and Weiner 1989; Perry 1989). During a certain period of *P. carterae* growth, the cells

form an elliptical ring structure composed of $CaCO_3$ crystals called coccolith, on the surface of the cells through the calcification. The formation of coccolith is synthesized in a special Golgi vesicle (Marsh 1999a). The coccolith consists mainly of two parts (Fig. 1A), V unit and R unit (Young and Bown 1991). The outer-tube and distant-shield elements form the V unit (Fig. 1B) and the R unit is a combination of the inner tube and proximal-shield (Fig. 1C). The closed double disc construction is formed by alternating V and R units on the organic base plate; the V unit and R unit are not inter-grown, just interlocking (Marsh 1994). The formation of coccolith is related to the three acidic polysaccharides PS1, PS2 and PS3 (Marsh 1994; Outka and Williams 1971b; Van der Wal et al. 1983).

The angle between the outer unit of the V unit and the base plate is 60°; the distant-shield is almost parallel to the base plate (Marsh 1999a). For R unit, the proximal-shield is attached to the base plate and parallel to it; the inner-tube of R unit is inwardly angled to the base plate by approximately 50° (Fig. 1A) (Marsh 1999a). Nevertheless, there are some hypotheses on the functions of coccolith (Borowitzka 1977; Sikes et al. 1980; Winter and Siesser 2006): 1. Protecting the cells; 2. Changing light intensity; 3. Increasing cell size; 4. Increasing the cell sedimentation rate to maintain it in a fixed aqueous layer.

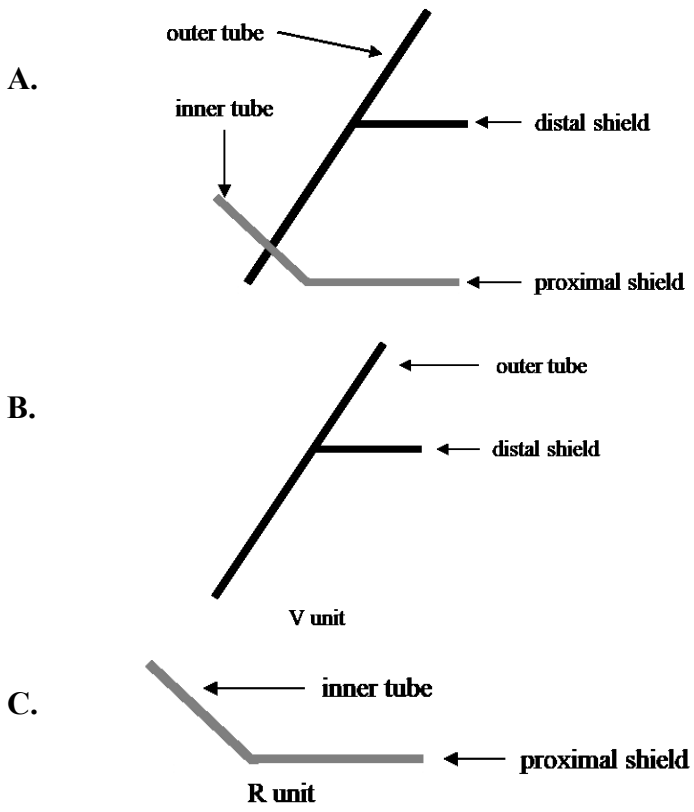

Fig. 1 Coccolith structure of previous research. **A:** V unit and R unit structure side view. **B:** V unit Side view. **C:** R unit Side view.

Because coccolith of *P. carterae* is thin and small, most of the coccolith SEM images are scattered and not very complete (Marsh 1999b; Marsh 2003; Walsh et al. 2018); However, In this study, we successfully observed a complete coccolith shell structure, which has not been reported previously.

Therefore, the purpose of this research is to discover the novel information of the structure and shape of the coccolith, advance the knowledge about the coccolith structure of *Pleurochrysis carterae* and the function of the $CaCO_3$ shell. In future experiments, we hope to perform an overexpression experiment on *P. carterae*, which requires the transfer of vector into the cell. However, the coccolith shell will block the vector from entering the *P. carterae* cell. So when we know the exact shell structure, we can find ways to

remove the shell of the surface without harming the cells.

2. Materials and Methods

2.1. Algal strain

Pleurochrysis carterae was purchased from National Center for Marine Algae and Microbiota (NCMA- https://ncma.bigelow.org/ccmp646) (Kindly provided by Dr. Fan Lu, Hubei University of Technology, China).

2.2. Preparation of f/2 medium

The f/2 medium contained 225 $mg \cdot L^{-1}$ $NaNO_3$, 5.6 $mg \cdot L^{-1}$ $NaH_2PO_4 \cdot H_2O$, 1 $ml \cdot L^{-1}$ trace metal solution, and 0.5 $ml \cdot L^{-1}$ vitamin solution (For other steps, refer to chapter II 2.2). The pH of the medium was adjusted to 8.5 after the configuration is complete.

2.3. Algal culturing

P. carterae were cultured in f/2 medium (Guillard and Ryther 1962). The starting cell density was 1.5×10^5 per liter. The culture temperature was set at 26 °C; the 16 h light and 8 h dark photocycle were provided by cool white fluorescent lights, and 24 h air pumping.

2.4. Scanning Electron Microscope (SEM) sample preparation

2.4.1. Sample fixation and dehydration procedure

The 2.5 % to 3 % concentration of glutaraldehyde in phosphate buffer (at a pH around 6.8 to 7.4) (Calvert et al. 1976) was prepared. The mature *P. carterae* cells were used as a sample. The 1 ml of *P. carterae* samples were placed into the glutaraldehyde solution for 30 minutes to ensure complete infiltration of the glutaraldehyde solution into the *P. carterae* to complete the fixation. The fixed *P. carterae* cells were subjected to gradient dehydration with 50 %, 60 %, 70 %, 80 %, 90 % and 100 % of ethanol, respectively, for

15 minutes at each concentration; The dehydrated algal cell samples were kept it in a -80 ℃ freezer until use.

2.4.2. Scanning Electron Microscope (SEM)

The dehydrated *P. carterae* cell samples were removed from the -80 °C freezer, then placed it into freezing-dryer (LABCONCO freezone 12, Kansas City, MO, USA) for 24 hrs. Cell samples were sputter coated the fully dried *P. carterae* cell samples with carbon powder and then imaged HITACHI SU-70 Scanning Electron Microscope to get the image.

3. Results

3.1. Novel *P. carterae* calcium carbonate shell structure

Unlike previous research results (Marsh 1999b), we found that on the top of the inner tube, there is a baffle structure which is with circular convex in shape (Fig. 2 and Fig. 3).

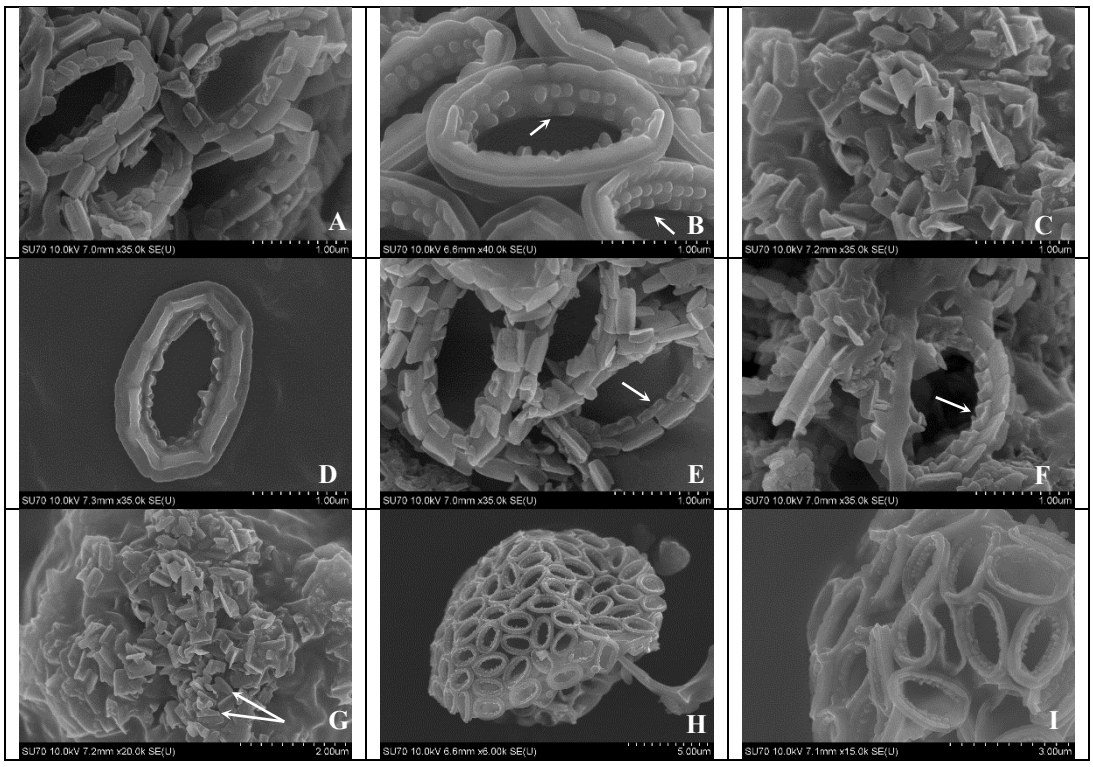

Fig.2 SEM pictures of coccolith. **A:** Loose structure of coccolith. **B, E, F:** The arrow

points to “doornail structure”. **C:** Cracked coccolith. **D:** Single coccolith. **G:** The arrow points to "R unit". **H, I:** *P. carterae* wrapped by coccolith.

Based on the observation, this structure is parallel with the outer tube of the V unit (Fig. 2 A, E, F). Because the shape of this round protrusion similar to doornail, we named this baffle structure the “doornail structure”. Based on previous research (Fig. 1B) (Marsh 1999b) and our results (Fig.2 B, C, E, F, G), we have built a new 3D model of coccolith, as shown in Fig. 3, and the side view of the newly discovered R unit and interlocking structure as shown in Fig. 4 A and B.

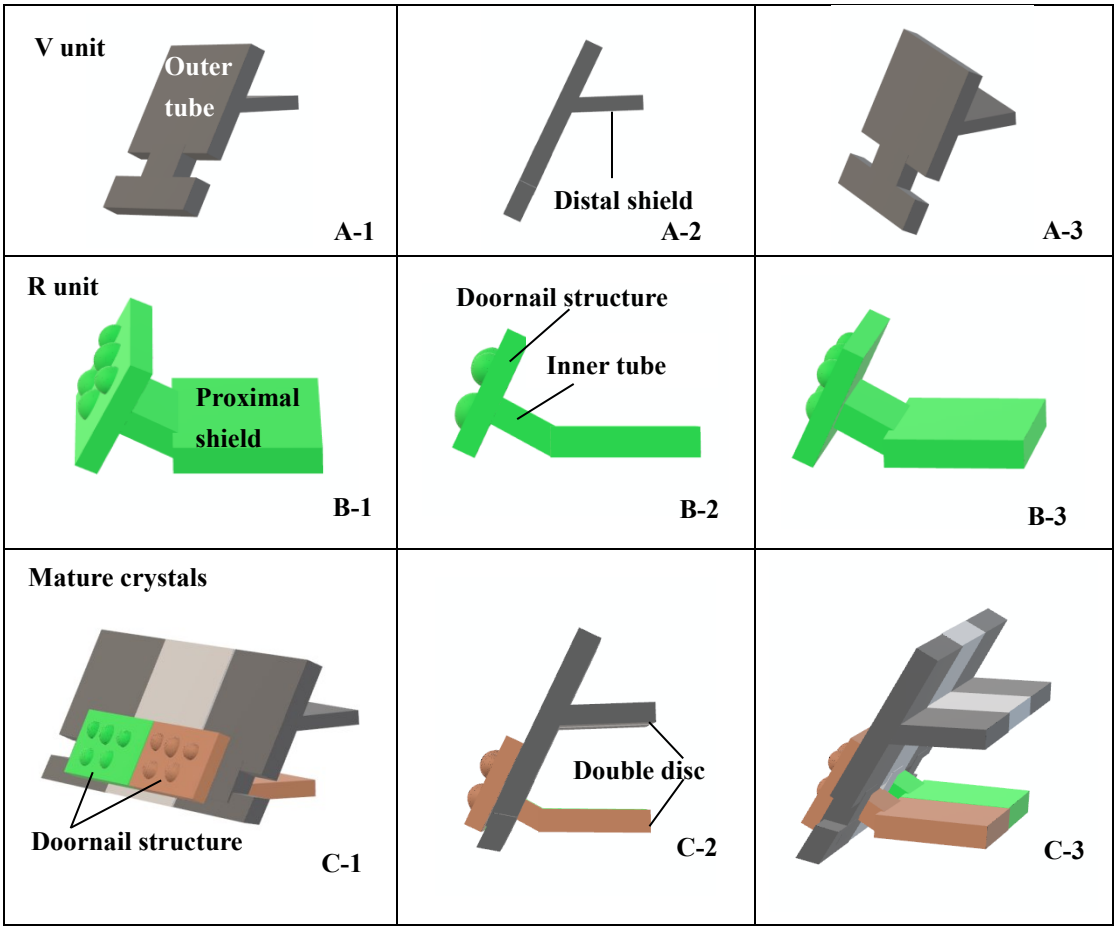

Fig. 3 The novelty discovered $CaCO_3$ shell 3D structure. **A-1**: Outer tube of V unit. **A-2**: Side view of the V unit and the distal-shield. **A-3:** 3D graph of V unit. **B-1:** Proximal-shield of R unit. **B-2:** Side views of the R unit include inner tube and doornail

structure. **B-3:** Updated 3D graph of R unit. **C-1:** Front view of the combination of V unit and R units.**C-2:** Side view of combination structure of V unit and R unit. **C-3:** Rear view of combination structure of V unit and R unit.

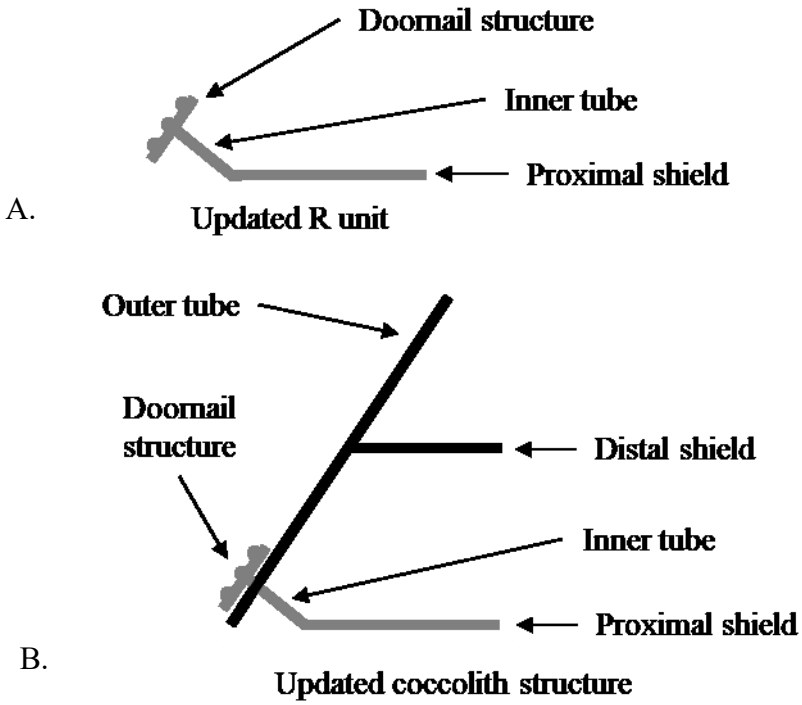

Fig. 4 The novelty discovered coccolith structure. **A:** Simplify graph of side view of R unit. **B:** Simplify graph of side view of combination structure.

3.2. Cross structure of coccoliths

We successfully found a complete coccolith shell. It can be seen in Fig. 5A; the protoplasts of *P. carterae* are no longer there, leaving only an empty shell, and it is not scattered. In Fig. 5E, the white arrow point to the distal-shield of the V unit and the black arrow refers to the proximal-shield of the R unit. It can be observed that distal-shield and proximal-shield are crossed together. The sample supporting structure graph is shown in Fig. 6.

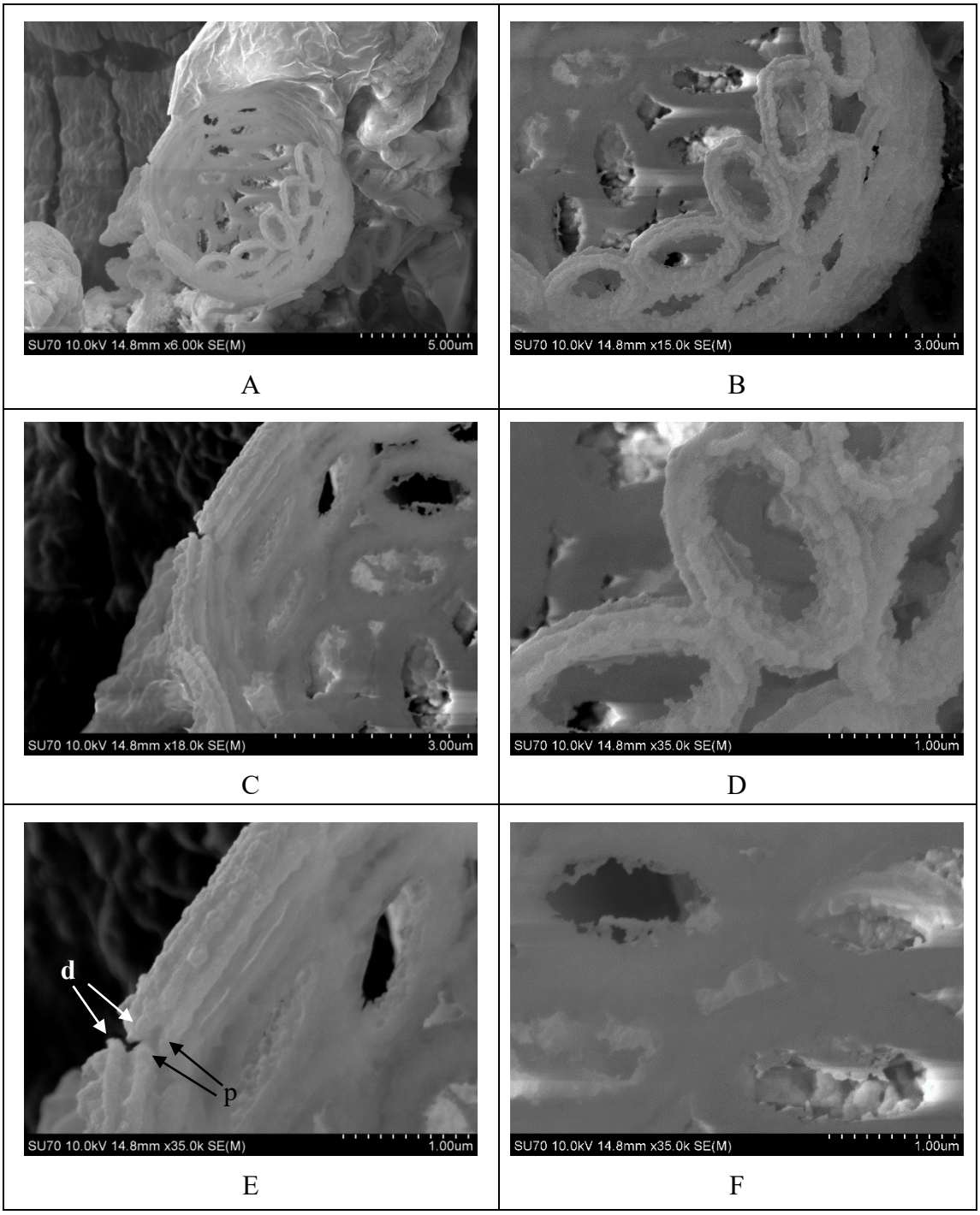

Fig. 5 SEM pictures of Support Structure of $CaCO_3$ cell wall. **A:** an empty shell without protoplasts. **B:** Close range view. **C:** Adjacent two coccolith side views. **D:** Top view of two adjacent coccoliths. **E:** Enlarged side view of two adjacent coccoliths. **F:** Rear view of several adjacent coccoliths. **Arrowhead d:** distal-shield. **Arrowhead p:** proximal-shield.

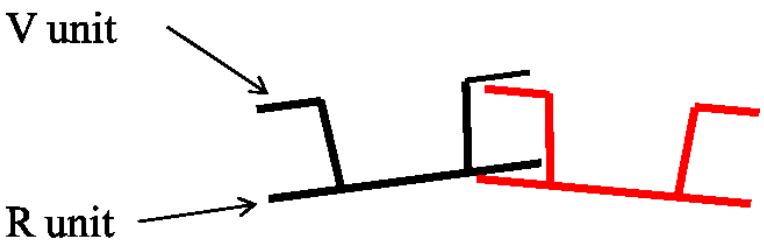

Fig. 6 Simplified schematic of the combination of two coccoliths.

Moreover, it can be observed the edges of the coccolith which are closed together (Fig. 5B, D, and F). From the above results, we presented a simple graphical structure of the entire shell which is shown in Fig. 7. The Fig. 7 shows that the double-disc edges of each coccolith are crossed together. These details of the coccolith structure on *P. carterae* have never been reported before.

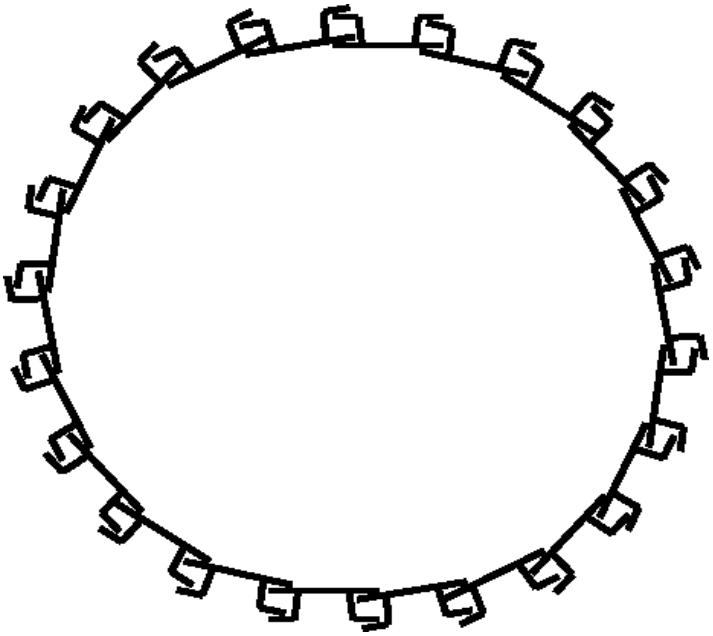

Fig. 7 Extracellular coccolith support structure/ Putative Support Structure of $CaCO_3$ cell wall

4. Discussion

Previous studies explained the structure of a single coccolith of *P. carterae* (Marsh 1999a; Marsh 2003), where R unit contains two parts, the inner tube, and the proximal shield. In

this experiment, when observing the surface calcification of *P. carterae*, a new structure was found (Fig. 2 and 3). This structure is connected to the inner tube, and the surface has obvious round bulges (Fig. 2B). It is parallel with the outer tube of the V unit. The overall shape is similar to the doornail, so we named it as "doornail structure". The complete coccolith structure is shown (Fig. 2 B and D), and it can be seen that the structure is very loose but not completely scattered, due to the presence of the doornail structure, the overall structure remained (Fig. 2 A and E). Thus, we speculate that the main role of this doornail structure in *P. carterae* is strengthening the overall structure of the coccolith and making it less prone to breakage. Also, the circular convex structures were speculated that it might have three uses: 1. making the doornail structure sturdier; 2. refracting the light which allows light to enter the cell better; 3. regulating the speed of water entering and leaving the cell.

Previous reports stated that the coccolith is a small structure, and it is easily damaged during the sample preparation process. Thus the complete structure cannot be observed (Marsh 1999b; Marsh 2003; Skeffington and Scheffel 2018; Walsh et al. 2018). There are very few related pictures illustrating how the *P. carterae* shell is supported. From our study, we are the first to observe and explain a complete shell structure of *P. carterae* (Fig. 5). From Fig. 5 we show that each of the coccolith's double discs crosses each other and they are fixed to each other like a bolt, which serves as a support fixing to ensure the integrity of the entire structure. Such a latch structure forms an outer shell of *P. carterae*. This result confirms that the coccolith plays a significant role in providing protection and support function to *P. carterae*. As single-cell phytoplankton, this scaly shell coccolith

has great flexibility. We suspect that during the cell division, the double discs of each coccolith could be gradually separate as the protoplasts expand, just like opening the bolts, thus, ensuring that the coccolith would not be damaged during the splitting process.

5. References

Beech P, Wetherbee R. (1984). Serial reconstruction of the mitochondrial reticulum in the coccolithophorid, Pleurochrysis carterae (Prymnesiophyceae). Protoplasma, 123:226-229

Borowitzka MM. (1977). Algal calcification. Oceanography and Marine Biology: an Annual Review-Pages, 15: 189-223

Calvert HE, Dawes CJ, Borowitzka MA. (1976). Phylogenetic relationships of Caulerpa (Chlorophyta) based on comparative chloroplast ultrastructure. Journal of Phycology, 12:149-162

Fabry VJ, Seibel BA, Feely RA, Orr JC. (2008). Impacts of ocean acidification on marine fauna and ecosystem processes. ICES Journal of Marine Science, 65:414-432

Guillard RR, Ryther JH. (1962). Studies of marine planktonic diatoms: I. Cyclotella nana Hustedt, and Detonula confervacea (Cleve) Gran. Canadian journal of microbiology, 8:229-239

Lowenstam HA, Weiner S. (1989). On biomineralization. Oxford University Press on Demand.

Marsh M. (1999a). Coccolith crystals of Pleurochrysis carterae: Crystallographic faces,

organization, and development. Protoplasma, 207:54-66

Marsh M. (1999b). Coccolith crystals ofPleurochrysis carterae: Crystallographic faces, organization, and development. Protoplasma, 207:54-66

Marsh M. (2003). Regulation of CaCO 3 formation in coccolithophores. Comparative Biochemistry and Physiology Part B: Biochemistry and Molecular Biology, 136:743-754

Marsh ME. (1994). Polyanion-mediated mineralization—assembly and reorganization of acidic polysaccharides in the Golgi system of a coccolithophorid alga during mineral deposition. Protoplasma, 177:108-122

Outka D, Williams D. (1971). Sequential coccolith morphogenesis in Hymenomonas carterae. Journal of Eukaryotic Microbiology, 18:285-297

Perry TG, Webb J, Mann S. (1989). Ferritin and hemosiderin: structural and magnetic studies of the iron core. Biomineralization: chemical and biochemical perspectives, 295-344.

Riebesell U, Zondervan I, Rost B, Tortell PD, Zeebe RE, Morel FM. (2000). Reduced calcification of marine plankton in response to increased atmospheric CO2. Nature, 407:364

Sabine CL et al. (2004). The oceanic sink for anthropogenic CO2. Science, 305:367-371

Sikes CS, Roer RD, Wilbur KM. (1980). Photosynthesis and coccolith formation: inorganic carbon sources and net inorganic reaction of deposition. Limnology and Oceanography, 25:248-261

Skeffington AW, Scheffel A. (2018). Exploiting algal mineralization for nanotechnology:

bringing coccoliths to the fore. Current Opinion in Biotechnology, 49:57-63

Van der Wal P, De Jong L, Westbroek P, De Bruijn W. (1983). Calcification in the coccolithophorid alga Hymenomonas carterae. Ecological Bulletins, 251-258

Walsh P, Fee K, Clarke S, Julius M, Buchanan F. (2018). Blueprints for the next generation of bioinspired and biomimetic mineralised composites for bone regeneration. Marine Drugs, 16:288

Winter A, Siesser WG. (2006). Coccolithophores. Cambridge University Press.

Young JR, Bown PR. (1991). An ontogenic sequence of coccoliths from the Late Jurassic Kimmeridge Clay of England. Palaeontology, 34:843-850

Young JR, Davis SA, Bown PR, Mann S. (1999). Coccolith ultrastructure and biomineralisation. Journal of Structural Biology, 126:195-215

CHAPTER V

Conclusions and future recommendations

1. Conclusions

With the acceleration of global industrialization, human's demand for energy is increasing. However, and the storage of traditional energy is very limited. It is extremely urgent to find new energy substitutes. Moreover, the combustion of fossil fuels produces a large number of greenhouse gases such as CO_2. To solve this problem, microalgae are considered to be a promising species for producing new energy and fixed carbon dioxide (Benemann 1997; Packer 2009). Among them, coccolithophore *Pleurochrysis carterae* has high lipid content (33 % of the dry cell weight) and can accumulate calcium carbonate on the cell surface through its unique calcification. Therefore, *P. carterae* have great potential for biodiesel production and fixing carbon dioxide.

In this research, *P. carterae* was used as experimental material, and several components were measured which could be affected by the different concentration of KNO_3 and NaH_2PO_4. Also, the structure of the *P. carterae* shell was studied. The experimental results are as follows:

1) The effect of NaH_2PO_4 on the components of *P. carterae* shows that:

   During the cultivation of *P. carterae*, 0.5, 1.5, 2 mM of NaH_2PO_4 could induce cells to secrete acidic substances in the early stage to lower the pH of the medium and reduce the synthesis of the intracellular lipids; 1.5 and 2 mM of NaH_2PO_4 inhibit the synthesis of calcium. However, 1.5 and 2 mM of NaH_2PO_4 can accelerate the proliferation of cells and enhance the content of chlorophyll α content.

2) The effect of KNO_3 on the components of *P. carterae* shows that:

When KNO_3 concentration was 0.75 $mmol \cdot L^{-1}$, *P. carterae* accumulated more calcium carbonate, around 10.01 % of dry weight. We also confirmed the accumulation of extracellular $CaCO_3$ by SEM. For coccolith accumulation, the SEM results were completely consistent with titration result, and KNO_3 could also affect the cell size of *P. carterae*. Moreover, within the range of 0, 0.25, 0.5, 0.75, 1 $mmol \cdot L^{-1}$ of KNO_3, The lipid and carbohydrate content of *P. carterae* were inversely correlated with the concentration of KNO_3. However, KNO_3 has a small promoting effect on the synthesis of proteins in *P. carterae.* To verify the results of lipid content, protein content, and carbohydrate content, the FTIR test was performed on day 10. The results of lipid, sugar and protein measurements measured by FTIR are consistent with previous experimental results.

3) The experimental results of the *P. carterae* shell show:

A new structure was found in coccolith. This structure is connected to the inner tube, and the surface has obvious circular bulges. Moreover, it is parallel with the outer tube of the V unit. The overall shape is similar to the doornail, so we named it as "doornail structure". Moreover, we first observed and explained the complete shell structure; the results show that each of the coccolith's double discs crosses each other and they are fixed to each other like a bolt. During this result, we confirm that the coccolith plays a significant role in provides protection and support function to *P. carterae.*

2. Future recommendations

Pleurochrysis carterae has great potential for numerous applications. Its main bioproducts are $CaCO_3$ and lipid. At present, in *P. carterae*, the highest yield of calcium carbonate can account for 10 % of dry weight (Jorquera et al. 2010; Moheimani 2005), while lipid production can account for 33 % of dry weight (Endo et al. 2016; Moheimani 2005). In the future, we are planning to increase the yields of the lipid and $CaCO_3$ by modifying the algae genome via genetic engineering. However, due to the lack of research on *P. carterae*, we are not clear about the genes which are related to biomineralization and lipid synthesis in *P. carterae*.

From the previous study of *E. huxleyi*, it can be known that V-ATPase participates in the intracellular calcification process of *E. huxleyi*, whose main function is transporting hydrogen ions (Mackinder et al. 2011). Base on the NCBI database, we found a gene fragment of the V-ATPase in *P. carterae*. We designed the primers for V-ATPase and performed the polymerase chain reaction (PCR) as shown in Figure 1. Primer sequences are shown in Table 1.

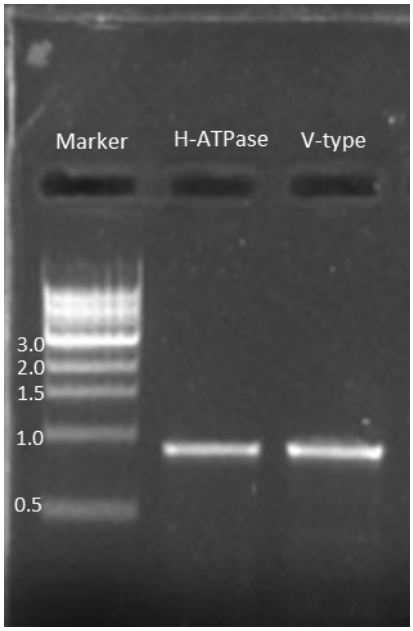

Fig. 1 Agarose gel electrophoresis results of H-ATPase and V-type

V-type ATPase	V-type _F	5’-GGATCCATGTCGGACCTCTGCCCGCCTACT-3’
	V-type_R	5’-AAGCTTGGAGCAAGGCGCCTCCTTGGAGG-3’
H(+)-ATPase	H-ATPase_F	5’- GGATCCATGTCGGACCTCTGCCCGCCTA-3’
	H-ATPase_R	5’- AAGCTTGGAGCAAGGCGCCTCCTTGGAG-3’

Table 1 Primer sequence of V-type and H-ATPase

From the above results, we know that we can obtain the target gene through the designed primers. Therefore, in future works, we can increase the expression level of V-ATPase to see whether the increase in V-ATPase expression level could affect $CaCO_3$ or lipid accumulation in *P. carterae* or not.

Until now, the whole genome sequence of *P. carterae* has not been reported yet, so in the future work, we are planning to sequence the whole genome sequence of *P. carterae*. Therefore, the gene sequence related to lipid synthesis or $CaCO_3$ synthesis could be found. Furthermore, we can find more valuable genes which could be used to enhancing the value of the algae, etc.

In our experiments, we also found that *P. carterae* can work with a bacterium to degrade phenol (Fig. 2).

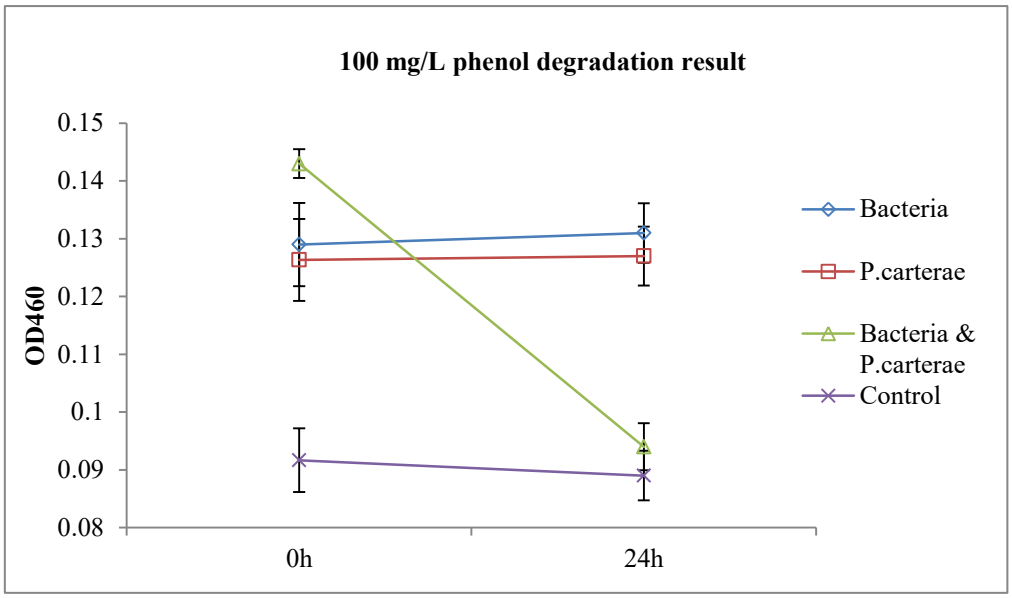

Fig. 2 Phenol degradation test

However, we are not sure what the relationship between the bacteria and *P. carterae* and it may be the following conditions:

1) The symbiotic relationship. Bacteria degrade phenol to provide nutrients for algae, while algae also provide the required nutrients for the bacteria.

2) The competitive relationship. Due to competition between the bacteria and algae, the bacteria or algae release a substance to kill each other, and this substance can degrade phenol.

We also identify bacteria by using 16s RNA sequencing. The primer we used are HAD-1 (5'-GACTCCTACGGGAGGCAGCAGT-3') as forward primer and E1115R (5'-AGGGTTGCGCTCGTTGCGGG-3') as reverse primer. According to the sequencing results, we know that the strain is *Nitratireductor sp.* So in future research, we can further explore how bacteria and *P. carterae* degrade phenol.

3. References

Benemann JR. (1997). CO2 mitigation with microalgae systems. Energy Conversion and Management, 38: S475-S479

Endo H, Yoshida M, Uji T, Saga N, Inoue K, Nagasawa H. (2016). Stable nuclear transformation system for the Coccolithophorid alga Pleurochrysis carterae. Scientific Reports, 6:22252

Jorquera O, Kiperstok A, Sales EA, Embirucu M, Ghirardi ML. (2010). Comparative energy life-cycle analyses of microalgal biomass production in open ponds and photobioreactors. Bioresource Technology, 101:1406-1413

Mackinder L, Wheeler G, Schroeder D, von Dassow P, Riebesell U, Brownlee C. (2011). Expression of biomineralization-related ion transport genes in Emiliania huxleyi. Environmental Microbiology, 13:3250-3265

Moheimani NR. (2005). The culture of coccolithophorid algae for carbon dioxide bioremediation. Murdoch University

Packer M. (2009). Algal capture of carbon dioxide; biomass generation as a tool for greenhouse gas mitigation with reference to New Zealand energy strategy and policy. Energy Policy, 37:3428-3437